Masters Degree in Chemical Engineering

Universidade do Porto

Faculdade de Engenharia

FEUP

Hydrogen from bio-alcohols:

An efficient route for hydrogen production via novel reforming catalysts

Foreign Institution Development Project

Nuno Ferreira

Marie Curie-Sklodowska University

July 2009

Acknowledgements

To the success of this project I cannot belt only to this last 5 months of work because everything I learn and what I am today as future engineering and principally as person I own to a diverse conjunct of factors and situations that lead a long with me these years of university student.

Seeing that, I must take in account the importance that every single person had on my academic life; to the ones that were since the beginning and to the others that I had the pleasure to meet through these years thank you for all moments that we passed together.

I want to thank to prof. Dr. hab. Andrzej Machocki and to Bogna Tomaszewska and Piotr Rybak for everything that they teach me and for the patience that they had with me answering to all my questions with the same will. I am thankful to them for creating me a warm and supporting environment in the laboratory.

To the people that worked with me the last 3 years in the students association of my faculty (AEFEUP) for helping me to grow as person and engineer and for all the patience on moments that tension and stress overcome everything else. To all of you, that easily passed from colleagues to real friends, a very special thanks.

To all my family, especially my parents, sisters and brothers-in-law, thank you for all the patience and support, fells good have the sensation that you will be always there for me.

Finally I have to say some words to some special friends without neglect all the mentioned before. To you, friends from life, Maria, Sérgio, and Ruben, you are the living proof that a true friendship can handle time and distance. To André Maia, one of the most intelligent people that I have the pleasure to met, thank you for all the help that you provide me without asking nothing in exchange. To you, Joana Pais, a person that still can surprise me every single day, thank you for being such a good friend and for having always a friendly word no matter what. And to “you” that I will never forget…

Abstract

The main goal of the whole project was the development of an active, selective, robust and low-cost catalyst for the production of hydrogen from bio-ethanol at low temperatures to be applied in small-scale fuel cell applications.

Five different cobalt-based catalysts, $CoO \therefore ZnO - Al_2O_3$ were synthesize by co-precipitation method with 10 to 50 cobalt wt% and tested in the steam reforming of ethanol a different temperatures between 350 and 600 °C.

The catalyst selected to be the one with better results in the pursuit of our goals was the one with 30 wt% of cobalt, showing a surface area of 95 $m^2.g^{-1}$ and mesoporous with an average of 19.26 nm. At 480 °C the catalyst exhibited the best results with no selectivity to ethylene, acetone and acetaldehyde; relatively lower selectivity to methane, around 8%; 100% conversion of ethanol and higher selectivity to hydrogen, values around 90%. Beyond having the lowest selectivity to carbon monoxide, around 5%, the amount produced is a little bit higher than the desirable to be used in PEMFC.

Keywords: Bio-ethanol; Cobalt-based catalyst; Hydrogen; Steam reforming.

Index

Abbreviations

FC – Fuel Cell

POx – Partial Oxidation

SRR – Steam Reforming Reaction

ATR – Autothermal Reforming

PEMFC – Polymer Electrolyte Membrane Fuel Cell

SRE – Seam Reforming of Ethanol

LC – Liquid Chromatography

GC – Gas Chromatography

BET – Brunauer-Emmett-Teller

MEA – Membrane Electrode Assembly

GDL – Gas Diffusion Layer

PAFC – Phosphoric Acid Fuel Cell

AFC – Alkaline Fuel Cell

MCFC – Molten Carbonate Fuel cell

SOFC – Solid Oxide Fuel Cell

PSD – Pore Size Distribution

BJH – Barrett-Joyner-Halenda

TPR – Temperature-Programmed Reduction

TCD – Thermal Conductivity Detector

FID – Flame Ionization Detector

SMR – Steam Methane Reforming

WGS – Water Gas Shift

1 Introduction

The lack of petroleum and the need to reduce the emissions of environmental pollutants and greenhouse gases arouse interest and open new horizons in order to find alternatives to the dependence on fossil fuel sources.

Due to his aptitude, as his capability of be produced from various primary renewable fuels and for being a clean burning fuel, hydrogen is gaining ground as a strong solution in the replacement of petroleum as an emission-free electricity in the future.

1.1 Hydrogen Production Techniques

In this context, and with wide progress on fuel cells (FC) technology, varied ways and techniques to produce hydrogen are being studying for the scientific community in order to try to adjust the production of hydrogen as profitable as it can be. They can be broadly classified into the followings sorts: Biological, where hydrogen can be produced, for instance, in an algae bioreactor by depriving the algae from sulfur [1]; Electrochemical, such as the electrolysis of water, by decomposition of H_2O molecule into O_2 and H_2 with an energy supply; and thermochemical, that includes partial oxidation (POx), steam reforming reaction (SRR), and autothermal reforming (ATR) of methanol, ethanol or other fuels.

Focusing more precisely on thermochemical techniques, POx consists in an exothermic reaction where the heat is provided by the partial combustion of hydrocarbons with oxygen; on the other hand SRR is an endothermic reaction involving hydrocarbons and steam. And ATR is thermally neutral and it combines both reactions, partial oxidation and steam reforming, in a measured ratio. POx and ATR reactions do not need a heated reactor as SRR however they require an expensive and complex oxygen separated unit. After a slight analysis between those methods, the SRR offers precise advantages over the others when used methanol or ethanol as reactants, especially when considering hydrogen yield and CO production [2]. Factor that need to be accentuated for the reason that the polymer electrolyte membrane fuel cells (PEMFC) are chemical delicate and they cannot tolerate, among others

common catalyst poisons, carbon monoxide on the feed, being only possible to work with minuscule levels such as less than 20 ppm [3].

1.2 Steam Reforming of Ethanol

In this thesis is focus into the steam reforming of ethanol (SRE) as a path to produce hydrogen for fuel cell applications. It is more attractive than use methanol since it is less toxic, is relatively easy and safe to store, transport and distribute and can be produced from biomass without net addiction of carbon dioxide to the atmosphere [4]. SRE, illustrated in equation (1), consists in an endothermic reaction of ethanol and water on a catalyst bed producing hydrogen and carbon dioxide.

$$C_2H_5OH(g) + 3H_2O(g) \rightarrow 6H_2(g) + 2CO_2(g) \quad (1)$$
$$\Delta H^{\circ}_{298} = 173.3\ kJ \cdot mol^{-1}, \qquad \Delta G^{\circ}_{298} = 65.0\ kJ \cdot mol^{-1}$$

The selection of a suitable catalyst plays a vital role in SRE for hydrogen production, so considering total decomposition of ethanol, it contains a carbon-carbon bond and as such requires a surface able to oxidize both carbon atoms to CO_2 and, simultaneously, it must not be active for the oxidation of H_2 to H_2O. A good catalyst should also maximize the hydrogen selectivity and ethanol conversion as well as inhibit coke formation and the production of undesirable products as CO and CH_4 among others [5]. In order to reach a catalyst with those characteristics and with the aim of enhance the activity and enlarge the surface area, a cobalt catalyst was promoted with two different metal oxides and formed a cobalt-based catalyst, $CoO \therefore ZnO - Al_2O_3$, that was used as catalyst bed on this experimental work. The oxide zinc offers a good reforming to obtain H_2 but from temperatures around 400 °C the surface area starts to get considerably lower. To contradict that effect an aluminium oxide was introduced into the catalyst bed; unfortunately as the aluminium prevent progress of reforming reactions, both oxides had to be careful used in ideal proportions.

A catalyst can be synthesized through different methods as impregnation, co-precipitation or hydrothermal synthesis; each method have different influences on catalyst proprieties and, consequently, on the reforming performance. In general, between this three methods, co-precipitation showed to be the best since it has better activity to hydrocarbon

conversion; higher surface area and H_2 yield (%) and a reasonable CO yield (mol %) to be applied in PEMFC[6]. Seeing that, the used catalyst was prepared by co-precipitation method. Two different processes were involved in this method: nucleation and growth. They exhibit significant differences at the equilibrium level such the nucleation requires a system far from the equilibrium and growth is a process that takes place in conditions which gradually approach the equilibrium state [3].

Chromatography is a technique that provides the separation and/or the analysis of the different compounds of a complex mixture. When a mixture of various components enters a chromatography process, the different ratios of migration for each component on the adsorptive materials will provide the separation. So, the biggest the affinity a molecule has for the stationary phase, most time it will spend in a column. Thinking about the physical state of the mobile phase, techniques can be separated into Liquid Chromatography (LC) and Gas Chromatography (GC), the first one has a liquid of low viscosity as mobile phase and the second one, an inert gas.

There are mainly three types of GCs: gas adsorption, which is commonly used to separate mixtures of gases and uses a comprised packed bed of an adsorbent as stationary phase; gas-liquid, where the separation is based on relative volatilities in a column of an inert porous solid coated with a viscous liquid; and capillary gas chromatography, a rapid method to separate mixtures that use glass or fused silica comprised in the capillary walls which are coated with an adsorbent [7]. In the present work the method used to identify qualitatively and quantitatively the products and side-products of the SRE was the capillary gas chromatography.

1.3 Hydrogen

Hydrogen is composed by a single electron around his atomic nucleus. It is the chemistry element most abundant in the universe however does not exist in his free form on earth appearing always connected with other elements. So, in order to obtain molecular hydrogen, H_2, is necessary to spend some energy in the dissociation of a primary source. Therefore hydrogen cannot be referred as a primary source but as an intermediary one.

More than be the most abundant, hydrogen is the one that has the higher rate of energy per unit of weight when comparing with other fuels as it can be seen in the figure (1.3.1) represented below:

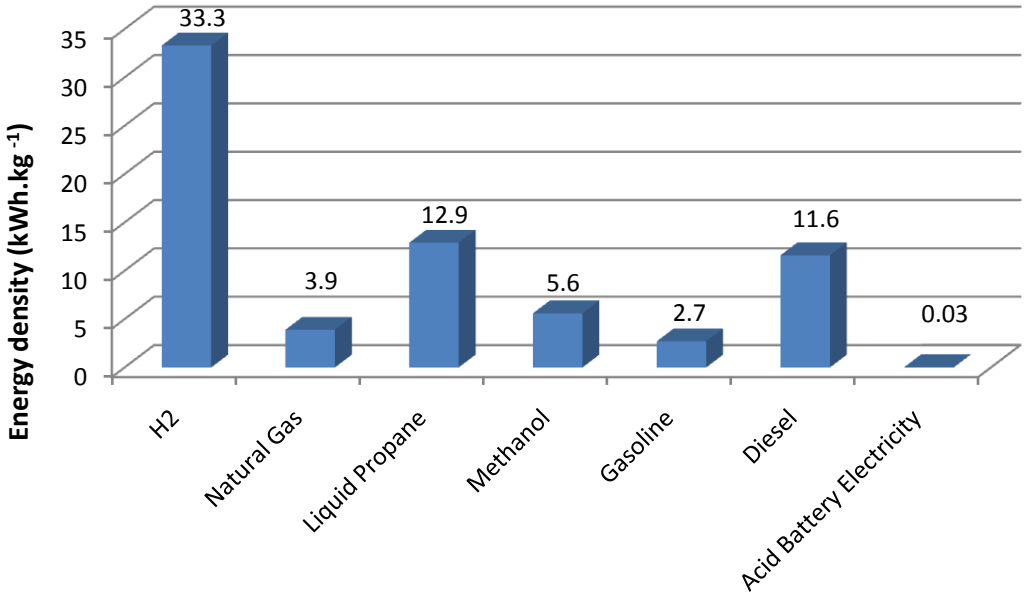

Figure 1.3.1 – Energy density per unit of mass for the different fuels.

However when compared the energy density per unit of volume, the situation is a quite different and hydrogen loses a lot to the other fuels.

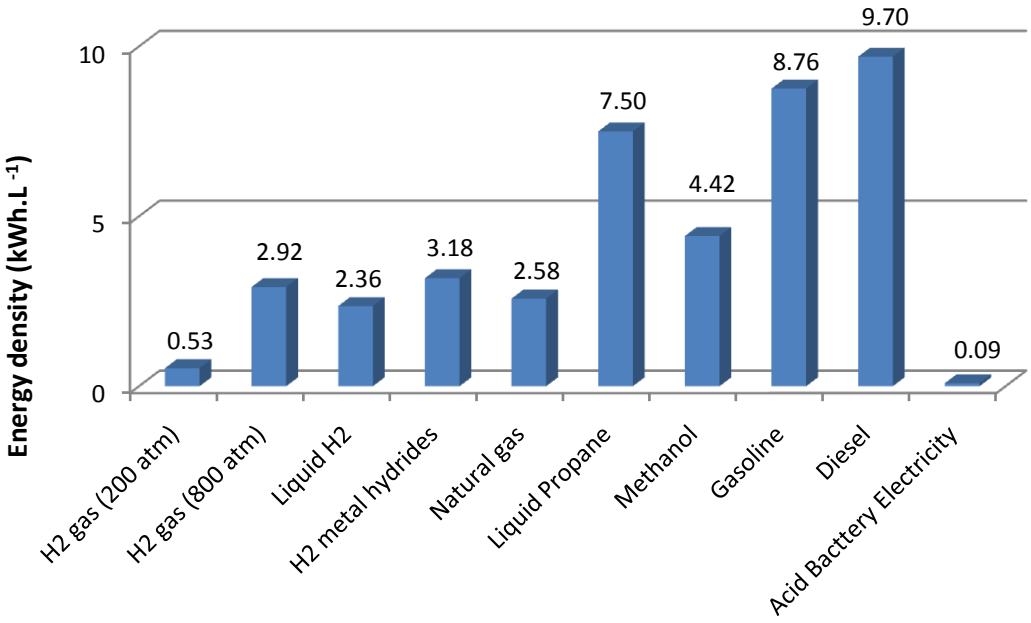

Figure 1.3.2 - Energy density per unit of volume for the different fuels.

As it can be seen beyond hydrogen has lower energy densities than the other fuels, around two or three times less, it will also depend on the way it will be stored and transported.

There are diverse ways to store hydrogen and the best choice will depend on the used transportation method, on where it will be applied and also the way that hydrogen economy will flow in the future.

Nowadays gaseous hydrogen can be compressed till 800 atm and transported in pressurized tanks but considerable amount of energy is required. As can be seen on the figure (1.3.2), the difference between hydrogen energy density from 200 to 800 atm is quite substantial. However for most mobile applications it is not enough and limits the operating range at least till the refuel of hydrogen be properly developed. It can also be transported in pipelines from the location of production till the location of consumption as in the case of natural gas but due to tiny size of his molecules, any small fissure or malfunction along the pipeline could end in gas leakage.

Hydrogen can be liquefied at minus 250 °C in return of a large amount of energy and despite the fact that it has a high complexity system of storage and refilling it could be the best way to use in automobile technologies.

It can also be stored in metal hydrides as magnesium or aluminium alloys that absorb the gas in their molecular structure. It offers higher volumetric energy density than the formers methods however the materials are too heavy and expensive and energy is needed to recover the gas.

As named above, there are many ways to store and transport hydrogen and much more that do not were mentioned. It is an economy with large margin of progression and many changes related with hydrogen will occur in the future.

Hydrogen has an awful reputation among general population when it concerns to handling it safely. It is a fear that is based on lack of information and due to limit knowledge and experience in his use. Furthermore it is a baseless fear since it cannot be forgotten that gasoline itself is both explosive and poisonous and people handle it every single day.

Assumption the worst case scenario, if a leak of hydrogen should occur, the chances of an explosion are small when assured proper ventilation since hydrogen mixes quickly with air to non-dangerous ratios. Comparing to common fuels used nowadays, hydrogen combustion release much less heat, burns much faster and his flame go up instead of spreading horizontally. So, in case of an accident, the damage from a hydrogen fire should be less serious than one from hydrocarbons.

1.4 Fuel cells – theory and types

A fuel cell is an electrochemical energy converter which, as his name says, convert chemical energy to electrical power by electrochemical reactions. It has a low degree of pollution and a high theoretical efficiency that can be expressed by the relation between chemical energy available and the higher heating value of FC reaction, as demonstrated below:

$$\eta = \frac{\Delta G}{\Delta H} \tag{2}$$

where ΔG and ΔH are respectively the free energy and enthalpy change of FC reaction. For electricity produced from chemical energy by fuel combustion, the efficiency is limited by operation temperatures, equation (3):

$$\eta = \frac{\mathrm{T_{max}} - \mathrm{T_{min}}}{\mathrm{T_{max}}} \tag{3}$$

This is known as the Carnot limitation and can be understood giving the example of a combusting engine in a driving car. Thus at high speeds, the engine is in his high-efficiency range, however at lower speeds or when it is constantly starting and stopping like it happens in city traffic, it reach the lowest efficiency promoting large amounts of pollution. The same example applied to a FC would be almost the opposite insofar as at lower loads it has the higher efficiency and with constant loads it will also have highly efficiency.

However the efficiency of a fuel cell demonstrated in equation (2) was merely theoretical and had the purpose of be compared with Carnot efficiency, giving that way a general idea. As a matter of fact losses related with activation, flow resistance, mass

transporting, fuel crossover and internal currents happens in a FC device. The last ones, fuel crossover and internal currents, are the most significant and are due to some flow of fuel and electrons through the electrolyte membrane where only should pass ions. This “non-ideal” situation provokes a decrease in the operation voltage when comparing with the theoretical situation and the efficiency of a FC can be correctly expressed by equation (4):

$$\eta = \frac{\mathrm{E_{real}}}{\mathrm{E_{ideal}}} \tag{4}$$

with $\mathrm{E_{real}}$ as the operating cell voltage and $\mathrm{E_{ideal}}$ as the ideal cell voltage, that can be calculated from the available free energy:

$$\eta = -\frac{\Delta G}{n \cdot F} \tag{5}$$

where n is the number of electrons transferred in the electrochemical reaction an F is the Faraday constant.

A fuel cell has a simple constitution as it is composed only by a few single components demonstrated in figure (1.4.1)

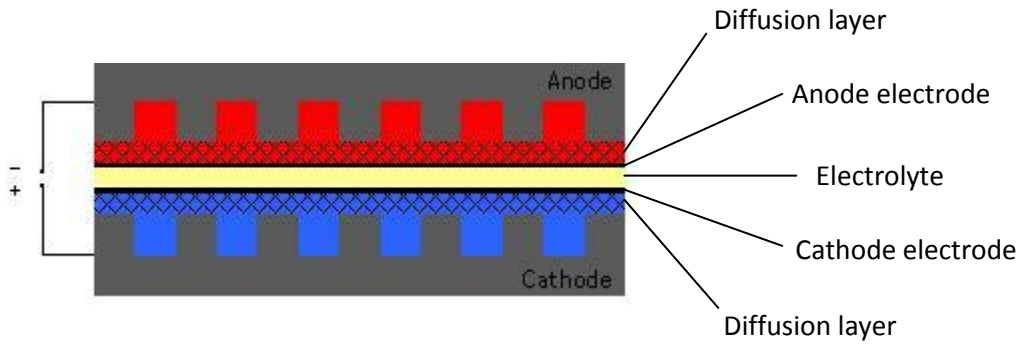

Figure 1.4.1 – Different components present in a fuel cell device.

The electrolyte or membrane is a component that has three main functions in a fuel cell: it acts as an electric insulator; conducts the ions from the anode to the cathode; and separates physically the two different electrodes. In the anode and cathode electrode surfaces occur the respective electrochemical reactions and the combination between the membrane and the electrodes is called of membrane electrode assembly (MEA). The gas diffusion layers

(GDL) are only used in low-temperatures FC and have the function of distribute the reactants to and remove the products from the respective electrodes. In order to ensure the distribution of the fuel and the oxidant, structures named flow fields are coupled, respectively, to the anode and cathode. These components can be composed by different materials and have varies structures depending on the fuel cell type.

The scheme described above is a single fuel cell, however to be able to develop systems of higher power, several cells are combined to form a stack. In these cases the flow-fields are called bipolar plates, and besides fulfill his primary function, it also combines the anode of one FC to the cathode of the other assembling the so-called stack.

Classifying the different types of FCs according their operating temperature we have two distinct groups: the low-temperature and the high-temperature fuel cells. In the first group it can be found the already mentioned PEMFCs that, as the name revel, use a solid polymer membrane as electrolyte. This membrane is chemically inert to reducing and oxidizing environments and is the component that limits the temperature in the entire device. Due to the low operating temperature, around 120 °C, it is required the presence of a noble metal as platinum in the electrodes which is the main problem related with the carbon monoxide concentration in view of the fact that it will poison the Pt electrocatalyst.

The following figure (1.4.2) illustrates in a simple way how a polymer electrolyte membrane FC works.

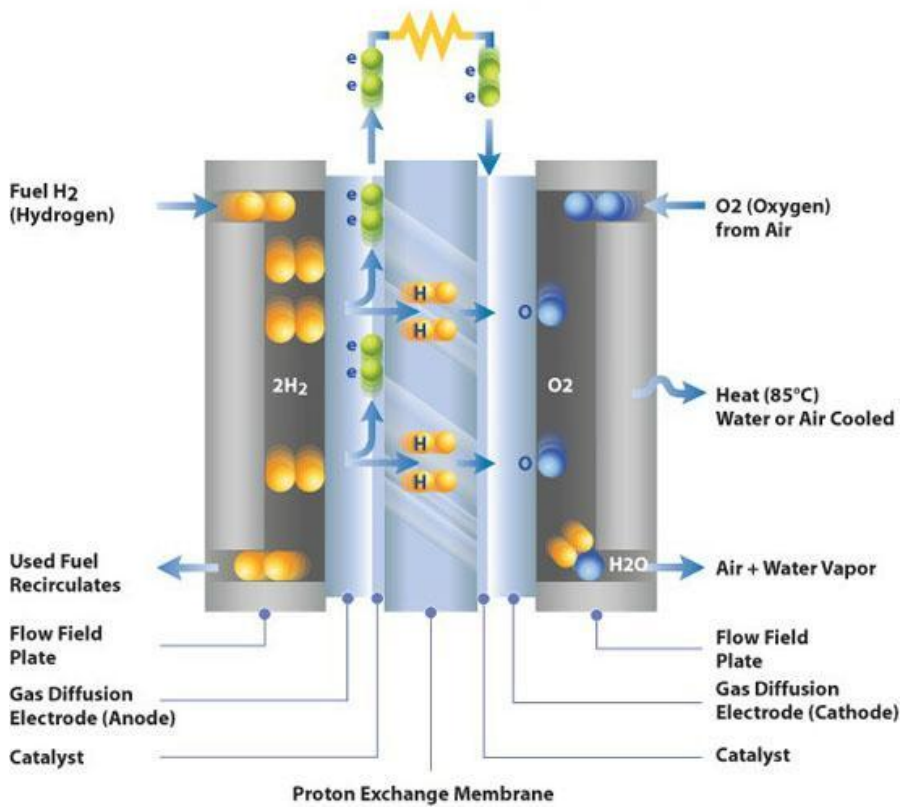

Figure 1.4.2 – Scheme of a PEMFC with the respective compounds.

As can be seen in the scheme exhibited above, the hydrogen is channeled through the flow field on the anode part of the cell where it will be split into positive hydrogen ions and negatively charged electrons. As the membrane is an electric insulator, it will only allow the positive ions passing through, forcing the electrons to travel along an external circuit creating the electrical current. At the same time that the hydrogen is supplied, oxygen (in air) is also channeled in the other side of the cell and will be combined with electrons and positive charged hydrogen to form water. This water is a key issue in PEMFC management since it will flood the cathode flow field and wet the membrane that has to be humid in order to work correctly.

The phosphoric acid fuel cell (PAFC) resembles to PEMFC in his constitution and way to work, however it operates at around 200 °C and uses concentrated phosphoric acid in a silicon carbide teflon matrix as electrolyte. Therefore and taking in account that this acid has a high freezing temperature, around 45 °C, it will lead to a longer start-up time and for being a poor ionic conductor at lower temperatures the poisoning of the platinum from carbon monoxide will increase.

This kind of FCs have a simple construction, are thermal, chemical and electrochemical stable and use a low volatile electrolyte, however when compared with other fuel cells systems they have lower power density and lower electrical efficiency.

Other type are the alkaline fuel cells (AFC), they work similar as the previous ones but with tiny changes with respect to the used electrolyte. It works in an alkaline environment using potassium hydroxide with concentrations between 35 and 50 wt% as electrolyte and the oxygen reduction is much faster than in acidic conditions making possible the use of a wider range of other cathodes. In this type, instead of hydrogen ions, the protons that act as conductive ions and pass through the membrane are the hydroxyl ions (OH^-). Due to this fact, the supply of oxygen has to be very pure for the reason that carbon dioxide will react with the electrolyte forming solid salts, altering the electrolyte properties. Thus common air cannot be used as feed of the oxidant and problems with cost-effective removal of carbon dioxide have limited the use of this fuel cell to special purposes like in submarines and spacecrafts.

In the high-temperature fuel cells group can be found the molten carbonate fuel cells (MCFC) that works at temperatures between 600 and 700 °C and the solid oxide fuel cells (SOFC) working at higher temperatures, around 1000 °C. Working at so elevated temperatures has great influence in the cathode kinetics, and make disappear the problem with carbon monoxide and dioxide in the feeds. However, the degradation of materials combined with the very corrosive used electrolytes, are an important issue when it comes to the selection of the material for his construction.

2 State of Art

2.1 Biological processes for hydrogen production

2.1.1 Biophotolysis of water by microalgae

A study made by Gaffrom and Rubin (1942) [9] focused on the mechanisms involved in hydrogen production by the enzyme hydrogenase, reached to two main conclusions: Unicellular algae which under anaerobic conditions and presence of light can reduce carbon dioxide, when placed in dark conditions and with air replaced by nitrogen, will slowly liberate hydrogen; When hydrogen and carbon dioxide are both absent of the photochemical reduction processes, the illumination of the fermenting algae enhances the liberation of hydrogen.

Another enzyme, nitrogenase, was study by Benemann and Weare (1974) [10] and was demonstrated that a nitrogen-fixing cyanobacterium produced hydrogen and oxygen in an argon atmosphere.

2.1.2 Hydrogen from photosynthetic bacteria

A photosynthetic bacteria undergo anoxygenic photosynthesis with reduced sulphur compounds as electron donors, was study by Miyake and Kawamura (1987) [11] as a potent hydrogen producer. According to them, the efficiency of light energy conversion to hydrogen is much higher than use a cyanobacteria.

2.1.3 Combined anaerobic and photosynthetic bacteria

Miyake et al. (1984) [12] proposed the combined use of photosynthetic and anaerobic bacteria for the conversion of organic acids to hydrogen, since the anaerobic bacteria produce hydrogen and organic acids from metabolized sugar but are incapable of

breaking down the formed acids by themselves. With the introduction of the photosynthetic bacteria, these acids can already be converted in hydrogen.

2.2 Electrochemical process for hydrogen production

Hofmann (1866) [13] invented an apparatus capable of electrolyzing water by joining three upright cylinders; the middle one open in the top to allow addiction of water; the other two, with a platinum electrode placed in the bottom and connected to the positive and negative terminals of a source of electricity. When current is run through the voltameter, oxygen forms at the anode and hydrogen at the cathode.

This is a well known process it can be used by different techniques but in industrial applications is rarely used, since hydrogen can be obtained more affordably by other processes.

2.3 Thermochemical processes for hydrogen production

The thermochemical processes for hydrogen production are the most common study and industrially used nowadays. It can be produced from various sources as methane, methanol or ethanol. However the ethanol is gaining ground as the most used reactant, mainly due to the lower CO production and the higher yield of H_2 that it can reach.

2.3.1 Partial Oxidation

It is a reaction that involves ethanol and oxygen with an appropriate molar ratio, up to 1.5, over a suitable metal catalyst with production of hydrogen and carbon dioxide as can be seen on the following equation (6):

$$C_2H_5OH(g) + 1.5O_2(g) \rightarrow 3H_2(g) + 2CO_2(g) \quad (6)$$

Mattos and Noronha (2005) [14] to investigate the effects of the supports nature in the product distribution on POx reaction, used a 1.5 wt% Pt loaded on Al_2O_3, ZrO_2 and $CeO_2 - ZrO_2$ supports prepared by incipient wetness. At 300 °C with a oxygen/ethanol molar ratio of 0.5, acetic acid was observed as a major product over Al_2O_3 supported catalysts and methane and acetaldehyde were observed on the others.

Sheng at al. (2002) [15] using 1 wt% Rh and 1 wt% Pt, loaded on CeO_2 support and prepared by impregnation method, temperature ranges between 200-900 °C and oxygen/ethanol molar ratio of 2, obtained the formation of large amount of H_2 by partial oxidation of ethanol.

2.3.2 Steam reforming

It is the reaction most commonly study worldwide, were made experiments with a large group of catalysts beds, prepared with different techniques and tested at diverse reaction conditions.

Lim et al. (2006) [16] using 12.5 and 21.5 wt% Co supported on ZnO, promoted by Na and prepared by co-precipitation in reactions at 500 °C and testing water/ethanol ranges between 5-13, concluded that higher Co loading and lower water/ethanol ratios, increased the ethanol conversion.

Cavallaro and Freni (1996) [17] using Cu, Ni and noble metals supported catalyst in a fixed-bed reactor at 100-600 °C and water/ethanol range between 6-10, concluded that the $Cu/ZnO/Al_2O_3$ catalyst exhibited better performance.

Diagne et al (2002) [18] using 2 wt% Rh supported on CeO_2, ZrO_2 and $CeO_2 - ZrO_2$, prepared by impregnation, in reactions with a water/ethanol molar ratio of 8 and testing temperatures ranges between 300-500 °C, concluded that the $Rh/CeO_2 - ZrO_2$ revealed better performance.

2.3.3 Autothermal reforming

This reaction can be broadly explained by the union of the two previous ones. In other words, when POx and SRR occurs simultaneously on the same catalyst bed, the exothermic heat generated in the first one can be used up *in situ* to drive the endothermic steam reforming reaction to a global thermally neutral reaction (eq.(7)).

$$C_2H_5OH(g) + (3-x)H_2O(g) + \frac{x}{2}O_2 \rightarrow (6-x)H_2(g) + 2CO_2(g) \quad (7)$$

The "*x*" factor is related with the water/ethanol and Oxygen/ethanol molar ratios, and is associated to the heating values of the reactants and products, in order to make the reaction thermally neutral.

Liguras et al. (2004) [19] used a 5 wt% $Rh/\gamma - Al_2O_3$ supported on cordierite monolith/ceramic foams and pellets, a water/ethanol and oxygen/ethanol respective molar ratios of 2-4 and 0.4-1.0. They conclude that the better performance was reached with the Rh supported on ceramic foams.

Cavallaro et al. (2003) [20] in order to study the effect of the different molar ratios on the catalytic performance, used a 5 wt% Rh supported on commercial $\gamma - Al_2O_3$ at 650 °C, a water/ethanol and oxygen/ethanol respective molar ratios of 2-3 and 0.2-1.1. They concluded that the addition of a small amount of O_2 increase the H_2 yield, reduces the coke and CH_4 formation and decrease the operating temperature.

3 Experimental methods

3.1 Co-precipitation

So as to obtain the catalyst by co-precipitation method the aluminum nitrate nonahydrate ($Al(NO_3)_3 \cdot 9H_2O$), Cobalt (II) acetate tetrahydrate ($Co(CH_3COO)_2 \cdot 4H_2O$) and zinc acetate dihydratate ($Zn(CH_3COO)_2 \cdot 2H_2O$) were weight based on previous calculations (see appendix A) and mixed in a reactor with approximately 250 cm^3 of water.

Table 3.1.1 – Amount to weight of each compound to synthesize the catalysts with different percentage of cobalt.

$\boldsymbol{Co\ (wt\%)}/_{\boldsymbol{Compound\ (g)}}$	$\boldsymbol{Al(NO_3)_3}$	$\boldsymbol{Zn(CH_3COO)_2}$	$\boldsymbol{Co(CH_3COO)_2}$
10	7.50	52.20	7.36
20	7.50	52.20	16.66
30	6.38	43.52	24.23
40	5.63	38.40	33.30
50	4.50	30.72	39.89

After check pH the precipitation starts, adding ammonium carbonate, $(NH_4)_2CO_3$, drop by drop on the mixture that was keep under non-stop mechanical stirring at 40 °C inside a reactor until the pH reach 8.5. Then it suffers heat treatment for about 30 min at 40 °C and 3 hours at approximately 55 °C always under stirring, in order to stabilize the deposit.

The precipitate passed for a filtration process in a Buckner funnel and washed with deionised water to diminish the existent ammonia. In order to reduce the amount of water as much as it could be done, it was washed with ethanol during the filtration and then distributed on ethanol and filtrated one more time.

The final steps of the method consisted in drying during 14 hours at 120 °C and calcination in a furnace at temperature of 400 °C during 6 hours, in this final step the deposit that was pink since the beginning of the process, turns to a dark green colour.

3.2 Catalyst characterization

On the characterization of the catalyst, to obtain Brunauer-Emmett-Teller (BET) specific surface areas, the total pore volume and pore size distribution (PSD) from Barrett-Joyner-Halenda method (BJH), was used a low temperature nitrogen adsorption in an ASAP – 2045 apparatus. In this equipment the samples had to be previous degasified during 2 hours at a temperature of 200 °C with the help of a vacuum pump to extract the gases. A static method of physic adsorption of nitrogen at 77 K was used to determine the adsorption-desorption isotherms, where the catalyst sample was exposed to nitrogen at different pressures up to 1 bar, which is the saturation pressure at that temperature, and the amount of nitrogen adsorbed was calculated based in a volumetric method.

3.3 Temperature-Programmed Reduction

The temperature-programmed reduction (TPR) is a technique used to analyze the reduction kinetics of oxide catalyst; it consisted in heating the catalyst with a linear temperature ramp, 10 °C.min^{-1}, while a 6% H_2-Ar mixture is passing through a quartz flow, 7 mm internal diameter, reactor with 0.05 g of catalyst (0.1-0.20 mm), at a flow rate of 30 cm^3.min^{-1}. The hydrogen consumption is monitored in order to obtain the profiles which will allow studying the influence of the support on the reducibility. The TPR was carried out in the apparatus AMI-1 (Altamira Instruments Inc.) and the water vapour formed during reduction was removed in a cold trap (immersed in liquid nitrogen-methanol slush, at -98 °C) placed before a thermal conductivity detector (TCD). The TCD was used to determine the amount of hydrogen consumed during temperature ramping and it signal was calibrated by injecting 55 µL of argon on the carrier gas.

3.4 Reactors set up

In order to obtain the hydrogen from the SRE, several fixed-bed continuous-flow quartz reactors, one for each concentration of cobalt in the cobalt-based catalyst, had to been built up. The previous preparation of the reactors has two different phases to concern about: first, the catalyst has to have some specific physic characteristics and second, the assembling of the reactor has a particular proceeding.

3.4.1 Preparing the catalyst

The catalyst, to be ready to use, needed to exhibit a diameter between 0,15 and 0,30 mm. Thus, with the help of a pestle, it was transformed in powder and then, as it was too small, a tablet was prepared in a hydraulic press (fig. 3.4.1.1) at 200 bar. Later than, with a spatula, it was divided in smaller pieces and the ones with the correct size were selected in a sieve.

Figure 3.4.1.1 – Hydraulic press used to prepare the tablets.

3.4.2 Preparing the reactor

The bottom of the small glass reactor, with 15 mm of diameter and 25 mm of height, was obstructed with quartz thread in order to later on do not let the inside compound fall down; but, in the same way, to let the ethanol go through. After that, quartz stones with

1,2 – 1,6 mm of diameter filling one layer or two helped on the stuck of the bottom of the reactor. Quartz stones with 0,3 – 0,6 mm were added till fulfill half of the reactor capacity and 0,1 g of catalyst was join and careful mixed with the smaller stones of quartz. This thinner quartz is used so that the catalyst does not compact, promoting good a contact and fluency of ethanol. In the end, the reactor was filled up with more small quartz, mixed again and assembled in an involucre to control the temperature of reaction.

(a) (b)

Figure 3.4.2.1 – Images of the reactor half filed (a) and totally filled (b).

3.5 Steam Reforming of Ethanol

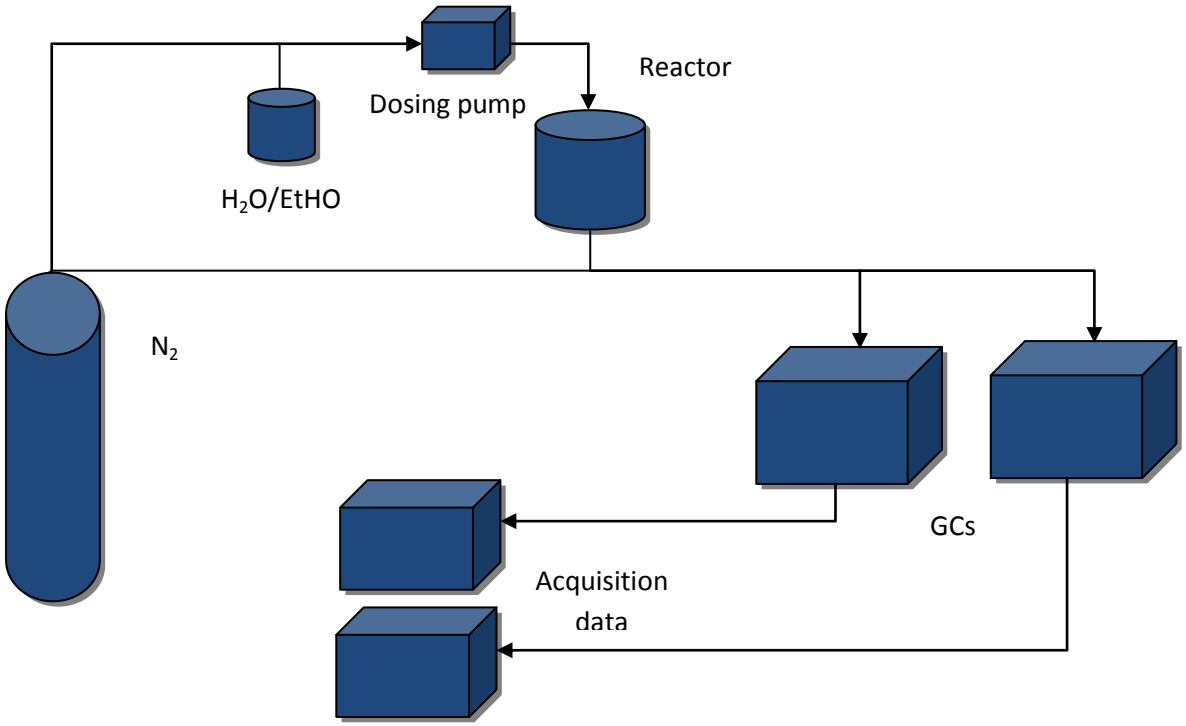

Figure 3.5.1 – Laboratory scheme of steam reforming of ethanol.

As the ethanol used was not bio-ethanol as it should be, was used a solution of ethanol with a proportion water/ethanol of 21:1 as it is found in bio-ethanol. This solution and the carrier gas, nitrogen, were fed at 25 and 75 $cm^3.min^{-1}$, respectively, by a dosing pump (Masterflex LS with 7013-20 head) both to a temperature controlled pre-heater unit. Unit that vaporize the ethanol solution to a pre-define temperature prior to reaction that occurs in a the temperature controlled reactor; several relative high temperatures from 350 to 600 °C were tested, to each catalyst, in order to conclude which is the most advantage way to produce hydrogen used in our specific goals. Prior to the steam reforming that was carried out under atmospheric pressure; all catalysts were reduced *in situ* with hydrogen during 1 hour at 350 °C.

3.6 Identification by Gas Chromatography

With the purpose of identify qualitatively and quantitatively the products of the SRE, were used two different gas-chromatography instruments, each one with affinity to specific compounds. Nitrogen was used as carrier gas and, before each catalyst analysis, the sensitivity of the detectors to the analysed compounds was calibrated with the single standard of that compounds.

For hydrogen measurements, was used the Gas-Chromatograph GCHF 18.3 equipped with a column packed with an activity charcoal. An average of 5 injections, with the endurance of 15 seconds each, was made for the different temperatures tested. The importance of fixing the injections times in one specific number is only to off-load one more variable in the all project context.

The Varian CP-3800, equipped with two different columns, flame ionization detector (FID) and TCD, was used to analyze the reaction side products and the non reacted reactants. This second GC had two different columns one filled with a porous polymer porapak Q to identify CO_2, C_2H_4, $(CH_3)_2CO$, non reacted H_2O and C_2H_5OH; and another with silica gel to identify the rest of the side products as CH_4 and CO and the carrier gas, N_2. For each temperature were made 2 or 3 injections being all the products identified by retention time.

4 Results and Discussion

4.1 Catalyst Characterization

In order to proceed to a good interpretation of the final results, the main surface properties of the different catalysts used had to be analyzed. Thus the followings figures represent the pore size distribution and the nitrogen adsorption-desorption isotherms for each catalyst.

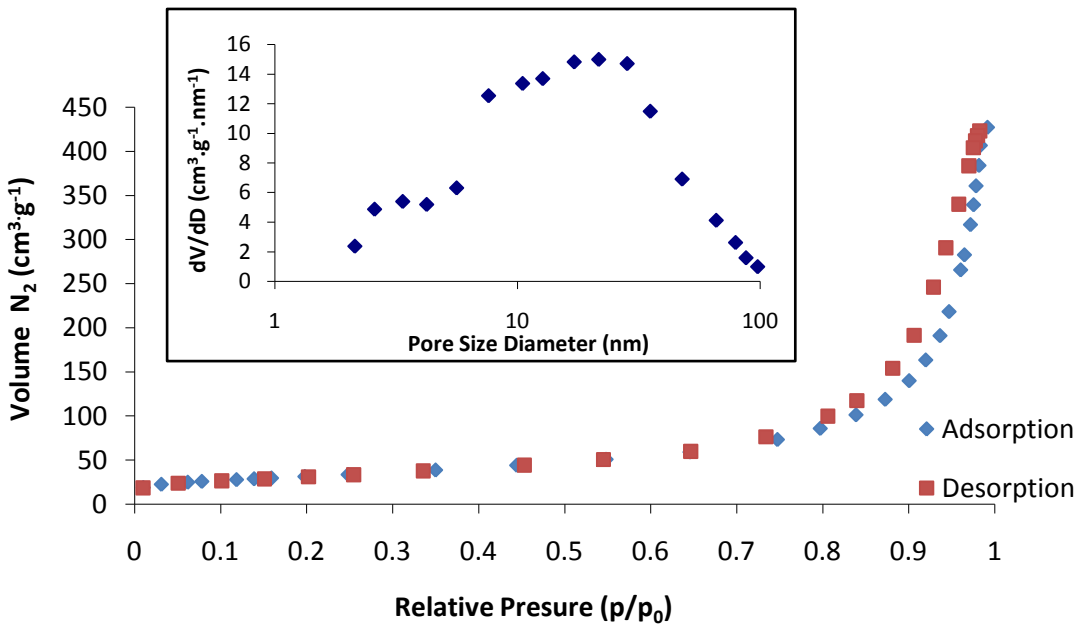

Figure 4.1.1 - PSD and N_2 adsorption-desorption isotherms to catalyst with 10 %Co.

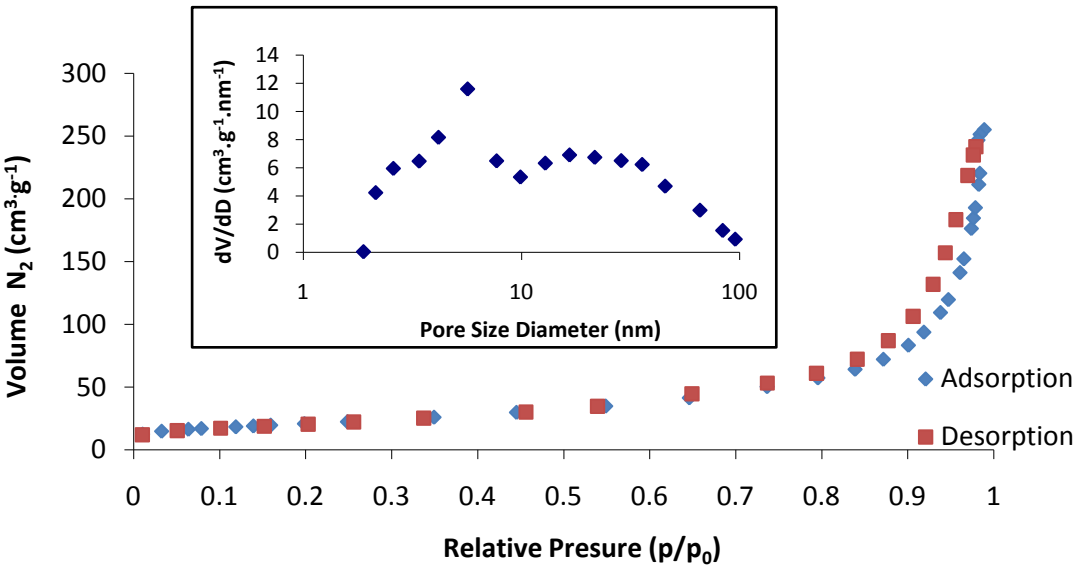

Figure 4.1.2 - PSD and N_2 adsorption-desorption isotherms to catalyst with 20 %Co.

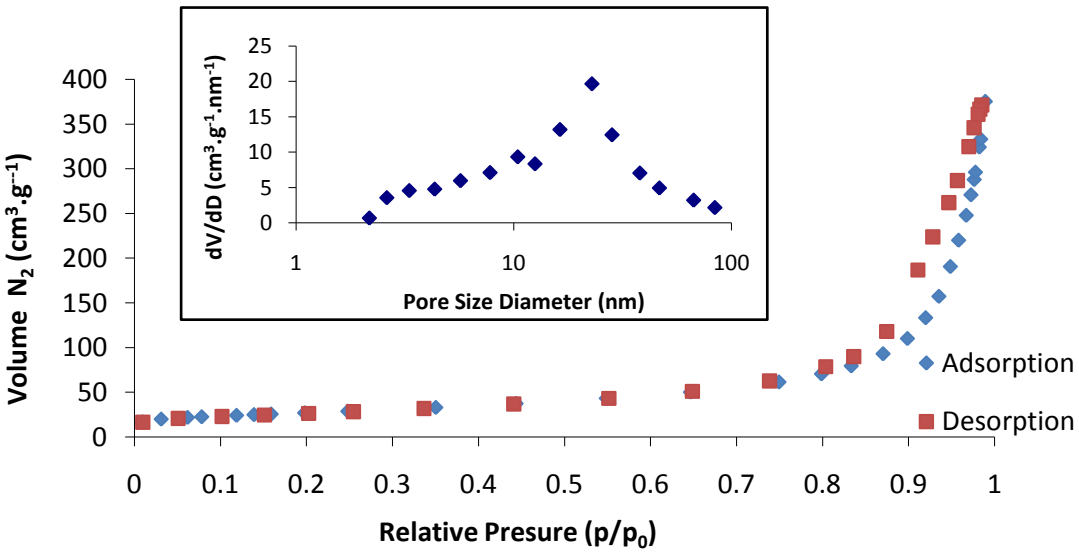

Figure 4.1.3 – PSD and N_2 adsorption-desorption isotherms to catalyst with 30 %Co.

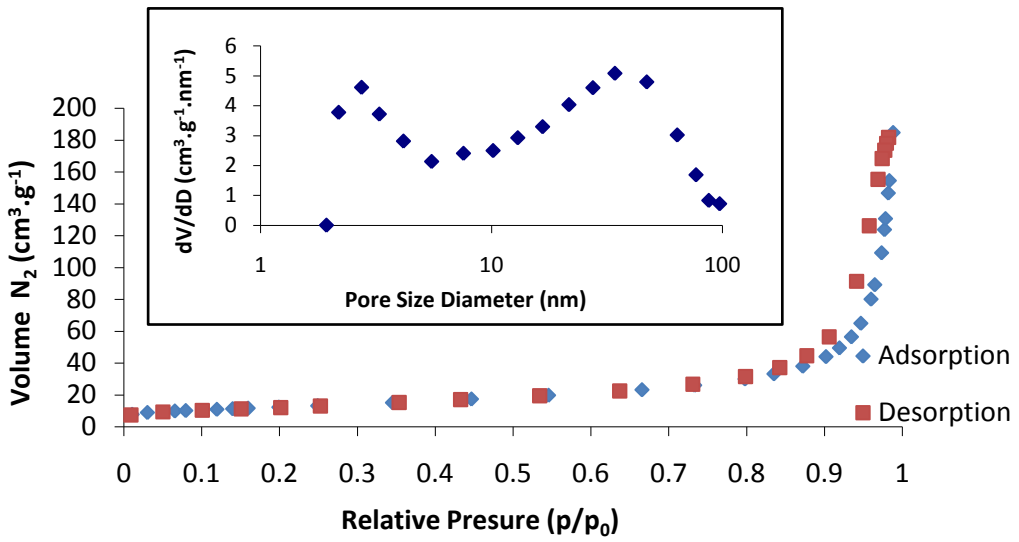

Figure 4.1.4 – PSD and N_2 adsorption-desorption isotherms to catalyst with 40 %Co.

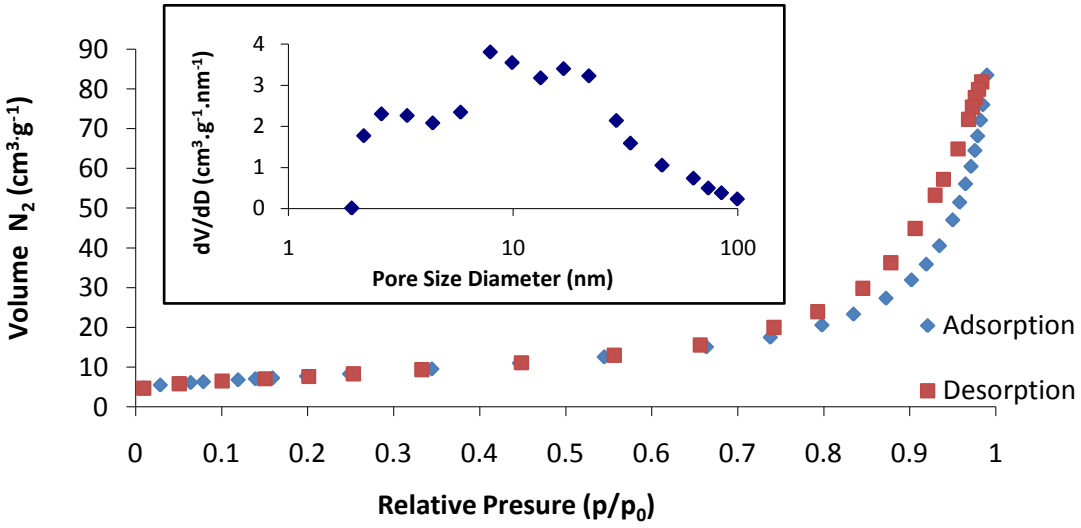

Figure 4.1.5 – PSD and N_2 adsorption-desorption isotherms to catalyst with 50 %Co.

Showed in the figures 4.1.1 to 4.1.5, is demonstrated a type-IV adsorption-desorption isotherms, with some interference of type-II. It can be seen that the process is linear almost since the beginning till fairly high relative pressures, almost 0.7, which is representative of type-II isotherms. For upper pressures it starts to demonstrate a behavior more exponential due the capillary condensation in mesoporous; however the amount of adsorbed do not rises

as sharply as it should be for a typical type-IV isotherm. The appearance of hysteresis loops is only typical of type-IV and type-V isotherms and is a phenomenon attributed to thermodynamic effects that lead to different pressures of capillary condensation and capillary evaporation. Isotherms like this, with type H3 loops that not level off at relative pressures near to the unit, are typical of material formed by aggregates of plate-like particles and give rise to slit-shaped pores.

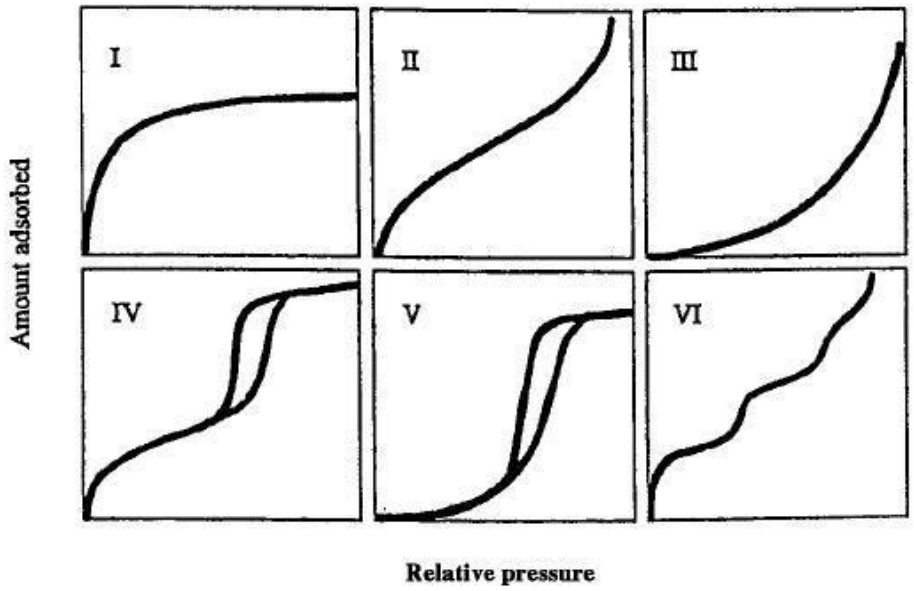

Figure 4.1.6 – The IUPAC classification for adsorptions isotherms.

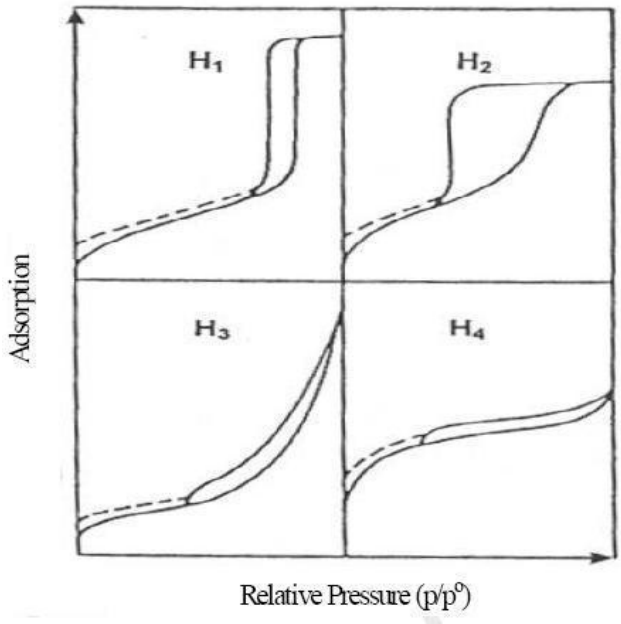

Figure 4.1.7 – The IUPAC classification to hysteresis loops in adsorptions isotherms.

The perfect situation would be achieve an adsorption-desorption isotherm type-IV without a horizontal level to relative pressures near to the unit indicating that the adsorption in all pores could be maximized and with hysteresis loops more likely type H1 where we have two vertical sections of the isotherm almost parallels, a factor that indicates the presence of pores with more regular shapes. In order to achieve this hypothetical situation silica could be combined with the catalyst to obtain those perfects isotherms; however this type of catalyst would have higher selectivity to ethylene.

Analyzing the PSD for the different samples and with the help of the table (4.1.1) that shows the surface area, the average pore diameter and total volume of pores, for each catalyst, we can conclude that the prepared catalysts are mainly mesoporous material, since the averages are between the 2 and 50 nm. The surface area decrease with the rise of the percentage of cobalt in the catalyst because it will occupy the space in porous and during calcination interactions between cobalt and the support, create a complex aggregate that will decrease his activity; however till 30% of cobalt the results obtained are agreeable with the expected, showing a surface area around the 100 $m^2.g^{-1}$. To catalysts with 40 and 50 % of cobalt, besides they do not have a satisfactorily surface area, during the filtration process, the water on the Buckner funnel come out with a pink hue that is characteristic of cobalt and means that not all cobalt reacted and, consequently do not precipitated.

Table 4.1.1 – Surface textural properties of the different cobalt-based catalysts.

Catalyst	Surface Area ($m^2.g^{-1}$)	Average Pore Diameter (nm)	Total Pore Volume ($cm^3.g^{-1}$)
10 %Co	112	18.22	0.6610
20 %Co	74	16.35	0.3949
30 %Co	95	19.26	0.5811
40 %Co	43	21.64	0.2858
50 %Co	27	14.58	0.1294

4.2 Temperature-Programmed Reduction

In the study of reducibility of the cobalt-based catalyst water is form in the process and it had to be removed because affect the reducibility of the catalyst by increasing the cobalt-support interaction and forming nonreducible cobalt aluminate.

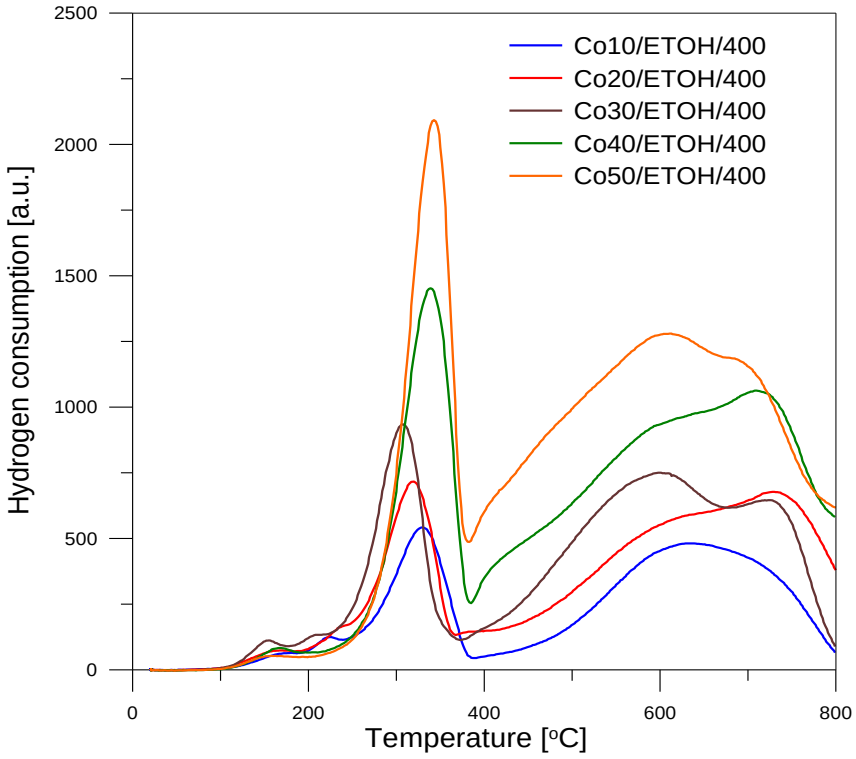

Figure 4.2.1 – H_2-TPR profiles of the different catalyst samples.

The H_2-TPR profiles for the different catalysts illustrated above (figure 4.2.1), exhibit two different peaks which indicate two different regions where reduction occurs. The first one a low-temperature peak between the 250 and 400 °C reaches the maximum rate of reduction at temperatures around 320 °C. This first stage of reduction can be interpreted as the formation of metallic cobalt from the cobalt oxide. The second region, a high-temperature peak, begins at 400 °C up to above the 800 °C. It interpretation is complicated due at the complexity of all reduction peaks and it can be associated to influences or interactions between the catalyst base.

Before the steam reforming, the catalysts were reduced *in situ* with hydrogen during 1 hour at 350 °C, this happens because the metallic cobalt increase the activity of the catalyst

4.3 Steam Reforming of Ethanol

Inside the reactor the main and most desirable pathway is the one that leaves to the SRE, equation (1), producing 6 mol of hydrogen and 2 of carbon dioxide from with 1 mol of ethanol and 3 of water. However, ideal situations are very difficult to achieve and side reactions happens with the appearance of some unwanted products.

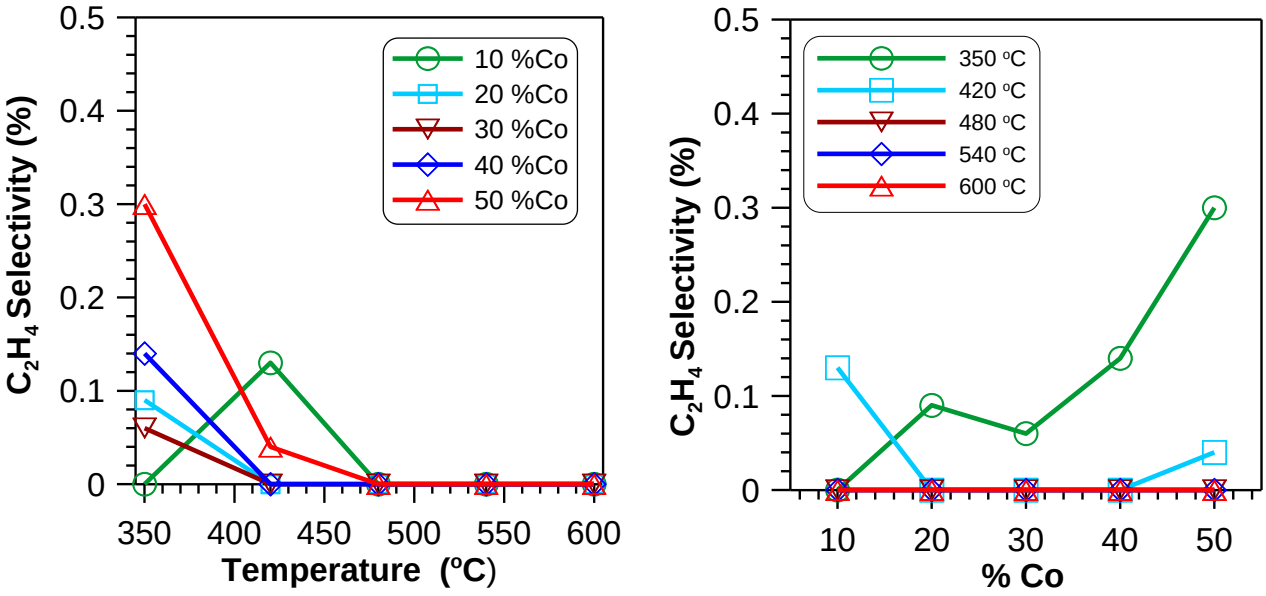

(a) (b)

Figure 4.3.1 – Effect of temperature (a) and cobalt wt% (b) in selectivity to ethylene in SRE.

In the figure (4.3.1) showed above we can see an example of a by-product, the ethylene; and the relation between his selectivity and the temperatures of reaction to the different catalysts

The main problems of side reactions are: that the by-products can give rise to reactions with harmful products to the equipments/environment or be already that kind of undesirable compounds; and, obviously, reduce the conversion of the main reaction, reducing

as well the production of the hydrogen. The selectivity of ethanol conversion into ethylene happens due the dehydration of ethanol as can be seen in equation (8).

$$CH_3CH_2OH(g) \leftrightarrow CH_2CH_2(g) + H_2O(g) \quad (8)$$
$$\Delta H^{\circ}_{298} = 45.4\ kJ \cdot mol^{-1}, \qquad \Delta G^{\circ}_{298} = 7.7\ kJ \cdot mol^{-1}$$

The formation of ethylene is not, for itself, a problem although it does not form any hydrogen that is the primary objective of this work so the less, the better. However the steam reforming of ethylene can compete with the SRE since it has an enthalpy slightly superior and is favored by higher temperatures.

$$CH_2CH_2(g) + H_2O(g) \leftrightarrow 4H_2(g) + 2CO(g) \quad (9)$$
$$\Delta H^{\circ}_{298} = 210.2\ kJ \cdot mol^{-1}, \qquad \Delta G^{\circ}_{298} = 114.5\ kJ \cdot mol^{-1}$$

This reaction produce a reasonable amount of hydrogen but has a big handicap, it produce 2 mol of carbon monoxide per mol of ethylene. The carbon monoxide has to be minimized at all costs because it poisons the platinum anodes of low-temperatures fuel cells as the PEMFCs which are the primary small-scale applications of the produced hydrogen.

So selectivity to ethylene has to be minimized and, as we can see in the graphics (fig. 4.3.1), the production of ethylene is reduced to zero at higher temperatures, since the 420 °C. The selectivity is slightly influenced for the amount of cobalt increasing proportionally mainly at the lowest temperatures. However in the all experience the maxim selectivity was around 0.3 % at 350 °C with cobalt with 50 wt%.

Methane is another of the by-products than has to be reduced to the minimum. When in presence of water, it also competes with the SRE with the steam methane reforming (SMR); reaction that, as the steam reforming of ethylene, has an enthalpy slightly superior than SRE being favored by higher temperatures.

$$CH_4(g) + H_2O(g) \leftrightarrow 3H_2(g) + CO(g) \quad (10)$$
$$\Delta H^{\circ}_{298} = 205.9\ kJ \cdot mol^{-1}, \qquad \Delta G^{\circ}_{298} = 142.0\ kJ \cdot mol^{-1}$$

This reforming is not convenient because, although the production of hydrogen in a molar ratio 3:1 to methane, it produce carbon monoxide, the most undesirable product in all process.

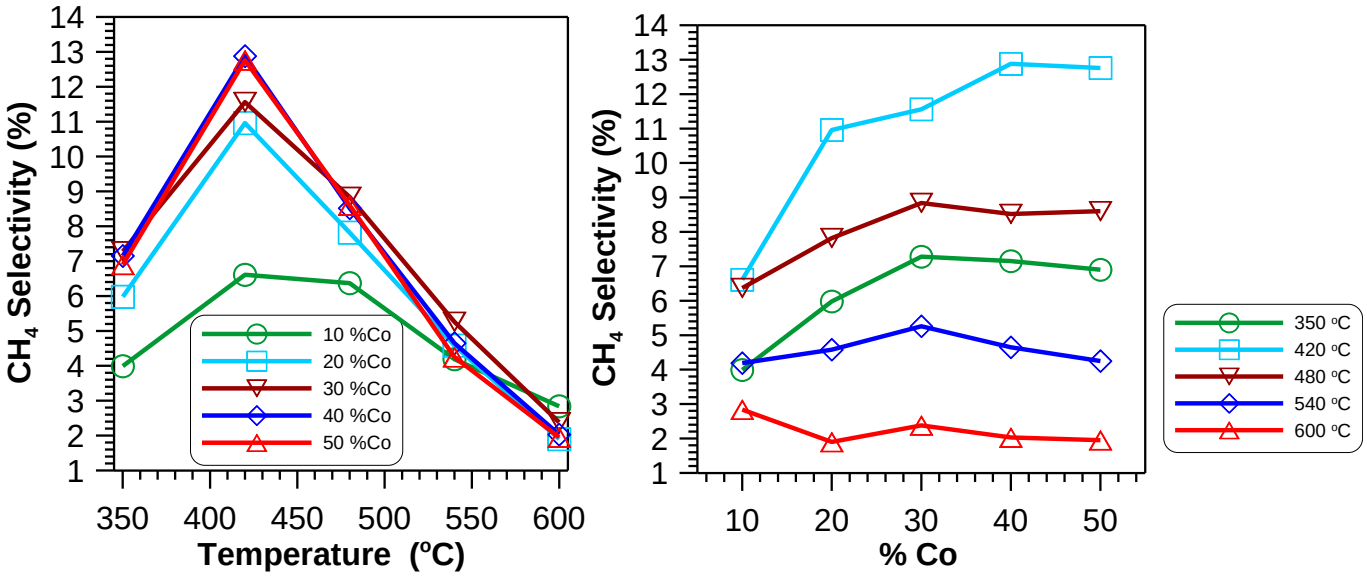

(a) (b)

Figure 4.3.2 - Effect of temperature (a) and cobalt wt% (b) in selectivity to methane in SRE.

Analyzing the effect of the cobalt wt % in methane selectivity we can see that it do not have much influence, being relatively constant along the rise of cobalt percentage with a small exception to the catalyst with 10 wt% to the temperature range of 350-480 °C revealing less selectivity to methane. However the temperature is a huge factor to concern about, since we have big discrepancies to the selectivity values between the different temperatures. At 420 °C exhibits the higher production of methane starting to drop substantially with the rise of the temperature. But at 350 °C occur a curious situation, being the one that shows the intermediate value among the 5 catalysts.

Acetone is another of by-products present on the steam of products from SRE. It is not harmful for the system but is unnecessary and, with its formation, the selectivity for hydrogen drops.

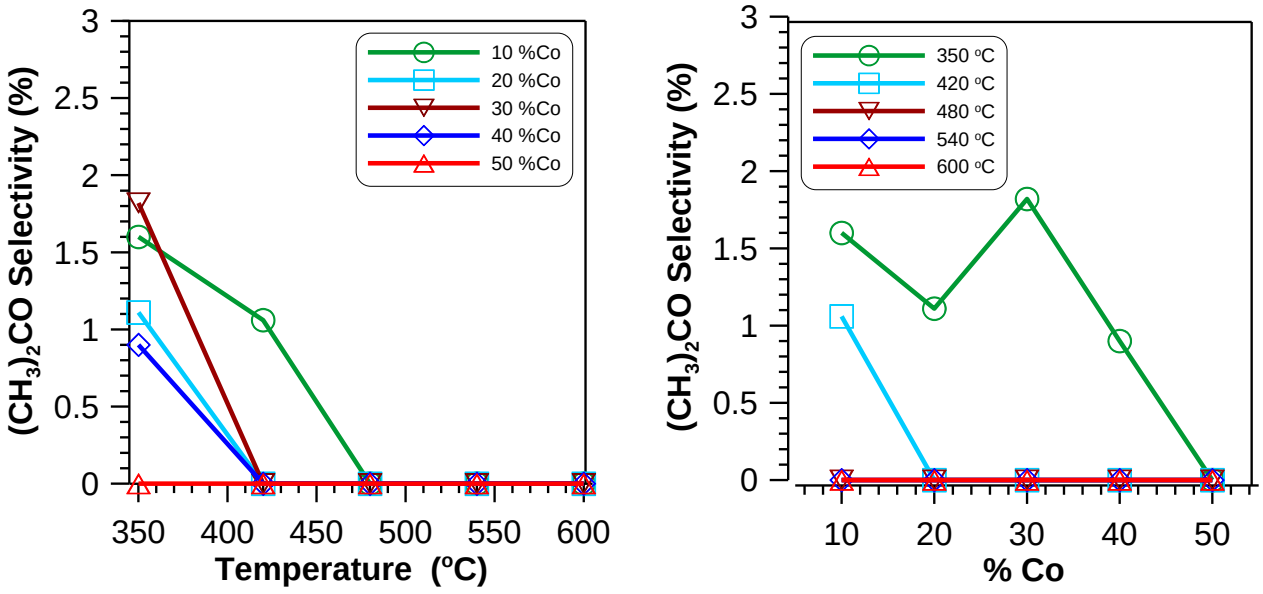

(a) (b)

Figure 4.3.3 - Effect of temperature (a) and cobalt wt% (b) in selectivity to acetone in SRE.

Acetone selectivity is favored for low temperatures being it formation totally depressed at temperatures higher than 480 °C. In order to try to understand the influence of the cobalt wt% we can focus on the variation of the selectivity at 350 °C. At that temperature, can be seen that the augment of wt% decrease the acetone selectivity but it is not so clear because at 30 wt% has the maximum of selectivity.

Acetaldehyde appears caused by the dehydrogenation of ethanol according to equation (11):

$$CH_3CH_2OH(g) \leftrightarrow CH_3CHO(g) + H_2(g) \quad (11)$$

$$\Delta H^{\circ}_{298} = 68.4\ kJ \cdot mol^{-1}, \qquad \Delta G^{\circ}_{298} = 34.7\ kJ \cdot mol^{-1}$$

Higher selectivity to acetaldehyde besides having a production of hydrogen six times less that the SRE, it has a bigger issue: his decomposition produces methane and carbon monoxide (equation (12)).

$$CH_3CHO(g) \leftrightarrow CH_4(g) + CO(g) \quad (12)$$

$$\Delta H^{\circ}_{298} = -18.8\ kJ \cdot mol^{-1}, \qquad \Delta G^{\circ}_{298} = -54.5\ kJ \cdot mol^{-1}$$

On the other hand, exists the possibility of the steam reforming of acetaldehyde, instead of his decomposition.

$$CH_3CHO(g) + 3H_2O \leftrightarrow 5H_2(g) + 2CO_2(g) \quad (13)$$
$$\Delta H^{\circ}_{298} = 104.8\ kJ \cdot mol^{-1}, \qquad \Delta G^{\circ}_{298} = 30.3\ kJ \cdot mol^{-1}$$

This situation is a good alternative to his decomposition and joined with equation (11) we can see that it is the SRE reaction in 2 different steps.

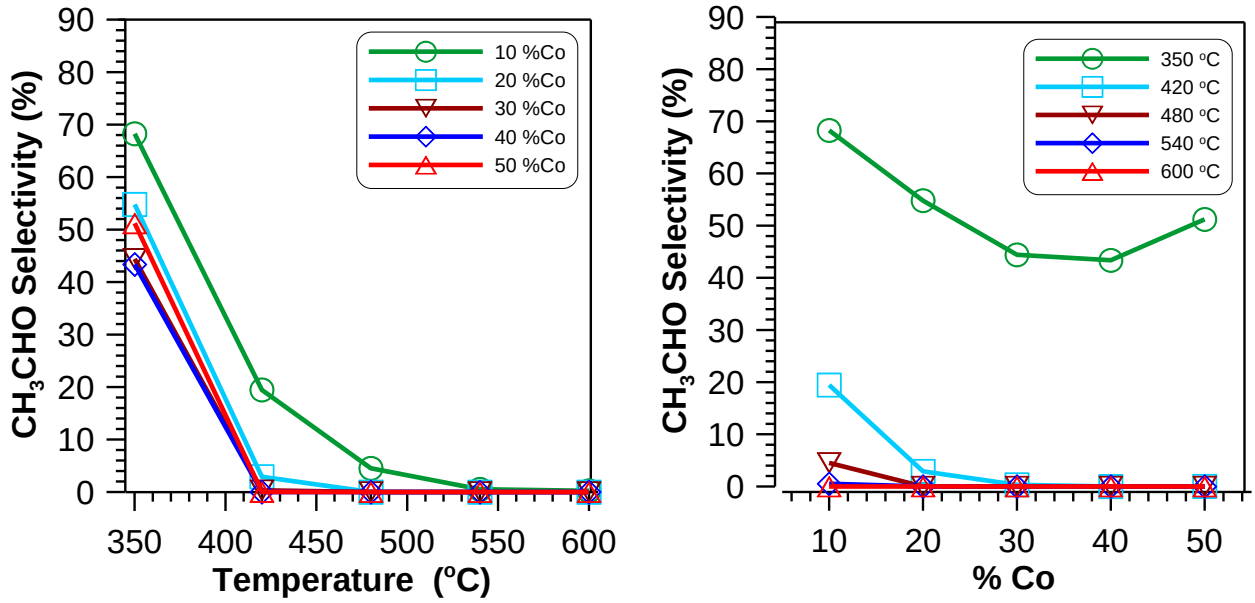

(a) (b)

Figure 4.3.4 - Effect of temperature (a) and cobalt wt% (b) in selectivity to acetaldehyde in SRE.

As it can be seen in the graphics showed above, figure(4.3.4), the amount of cobalt do not have significant influence on the selectivity of ethanol conversion into acetaldehyde, with a small exception on the 10-20 wt% at 420 °C where exhibits a drop from the 20 % to less than 10 %. However the temperature has an important role in this subject, in view of the fact that at 350 °C the selectivity is over the 40 % for all catalyst and in the next temperature, 420 °C, only with 10 wt% show signs of some selectivity, 20%, being totally depressed for further temperatures in all catalysts.

As was already explained, the carbon monoxide is the by-product that has to be avoided at all cost. In order to understand how it could be avoided we have to know how it is produced. In spite of all equations that were already mentioned and contributed for his formation, is one specific that is very important insofar as it could consume the carbon monoxide formed in the others side reactions.

$$CO(g) + H_2O \leftrightarrow H_2(g) + CO_2(g) \qquad (14)$$

$$\Delta H^{\circ}_{298} = -41.1\ kJ \cdot mol^{-1}, \qquad \Delta G^{\circ}_{298} = -28.6\ kJ \cdot mol^{-1}$$

This equation (14) has the name of water gas shift reaction (WGS) and, as it can be seen, consumes carbon monoxide in the same rate that forms hydrogen.

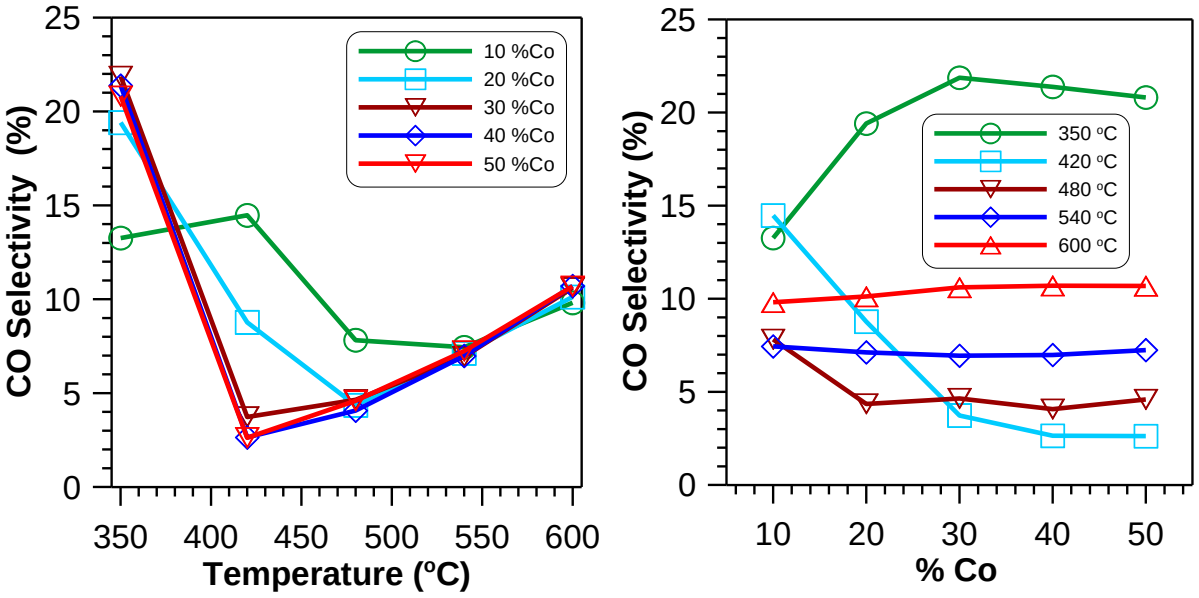

(a) (b)

Figure 4.3.5 - Effect of temperature (a) and cobalt wt% (b) in selectivity to carbon monoxide in SRE.

The selectivity to carbon monoxide is strongly related with the temperature; it have similar behavior to the different catalyst at the same temperature with the exception of 10 wt% at 420 °C that seems to be a little bit higher than it should, and could be an error of proceeding. The amount of carbon monoxide decrease with the augment of the temperature till values of 420-480 °C. Then starts to increase again for higher temperatures, but never reaches the higher values that have at 350 °C. The percentage of cobalt has slight influence in

the selectivity being essentially the same with the increasing of the wt%; although tiny exceptions occur between the 10 and 20 wt% at the lowest temperatures.

The appearance of carbon dioxide has many explanations as it have been demonstrating along of this work. However the most important is the one that is related with the WGS reaction. It will be fair to think that producing large amount of carbon dioxide could be prejudicial to the environment, but seeing that it consumes the carbon monoxide and analyzing that is used biomass-derived ethanol, we can conclude that the amount produced in the SRE and WGS reactions is essentially the same used to produce glucose by photosynthesis. Therefore this same glucose, will give origin to the ethanol used in SRE.

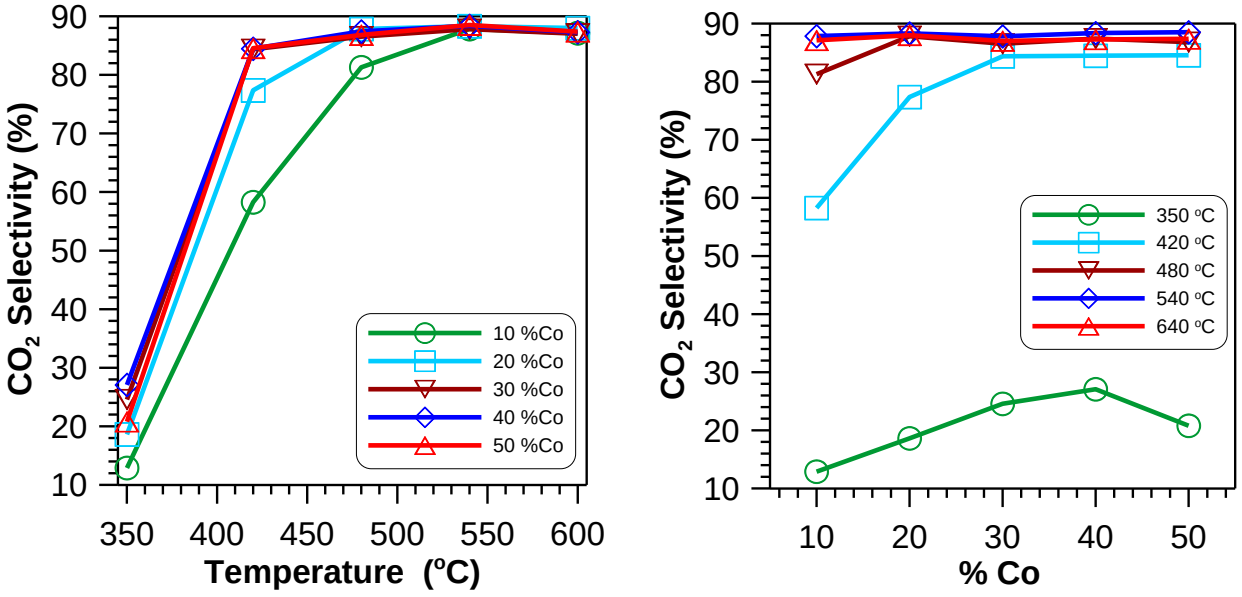

(a) (b)

Figure 4.3.6 - Effect of temperature (a) and cobalt wt% (b) in selectivity to carbon dioxide in SRE.

Observing not only the graphics to carbon dioxide selectivity, figure (4.3.6) but also the ones to carbon monoxide, figure (4.3.5) a relative inverse proportionality can be seen and is based in the WGS reaction. Contrarily to carbon monoxide, the selectivity for carbon dioxide increase with the temperature, reaching a landing at 480 °C with 90 % of selectivity. Moreover a huge raise is exhibit between 350 and 420 °C for all catalysts. The quantity of cobalt in the

catalyst is not an important factor to the selectivity, only to smaller percentages a significant difference can be noted, mainly to the lowers temperatures.

The ethanol conversion is much higher than the conversion for water (fig. 4.3.7). It mainly happens because of two separated phenomenon. The first one is connected with the side reactions that occur without the participation of water; reactions with selectivity to by-products already mentioned and to the ethanol decomposition exemplified on equation (15):

$$C_2H_5OH(g) \rightarrow H_2(g) + CH_4(g) + CO(g) \quad (15)$$
$$\Delta H^{\circ}_{298} = 49.7\ kJ \cdot mol^{-1}, \qquad \Delta G^{\circ}_{298} = -19.8\ kJ \cdot mol^{-1}$$

the resultant products of this reaction are hydrogen, methane and carbon monoxide, and as we can deduce, it is not a god pathway to follow, since it has two very undesirable by-products and a lower rate of hydrogen production.

The other reason to a lower conversion of water is related to his excess in comparison with the reforming stoichiometry. For other words, is used a molar ratio of water/alcohol of 21:1 in the fed of the reactor to simulate the use of bio-ethanol but the molar ratio of the SRE reaction is 3:1. The higher ratio used more energy as to be spent to generate extra steam. However water used in excess can be useful because contribute to WGS reaction and, in case of dehydrogenation of ethanol to acetaldehyde (equation (11)), excess of water will favour the reforming with a molar ratio 3:1 (equation (13)) instead of the reforming with a 1:1 molar ratio:

$$CH_3CHO(g) + H_2O \leftrightarrow 3H_2(g) + 2CO(g) \quad (16)$$
$$\Delta H^{\circ}_{298} = 187.1\ kJ \cdot mol^{-1}, \qquad \Delta G^{\circ}_{298} = 87.5\ kJ \cdot mol^{-1}$$

the same reasoning can be applied to the SRE, that with a molar ratio of 1:1 has similar behavior:

$$CH_3CH_2OH(g) + H_2O \leftrightarrow 4H_2(g) + 2CO(g) \quad (17)$$
$$\Delta H^{\circ}_{298} = 255.5\ kJ \cdot mol^{-1}, \qquad \Delta G^{\circ}_{298} = 122.2\ kJ \cdot mol^{-1}$$

In both situations the hydrogen produced is lower than with higher ethanol/water molar ratios and instead of carbon dioxide we have the formation of carbon monoxide.

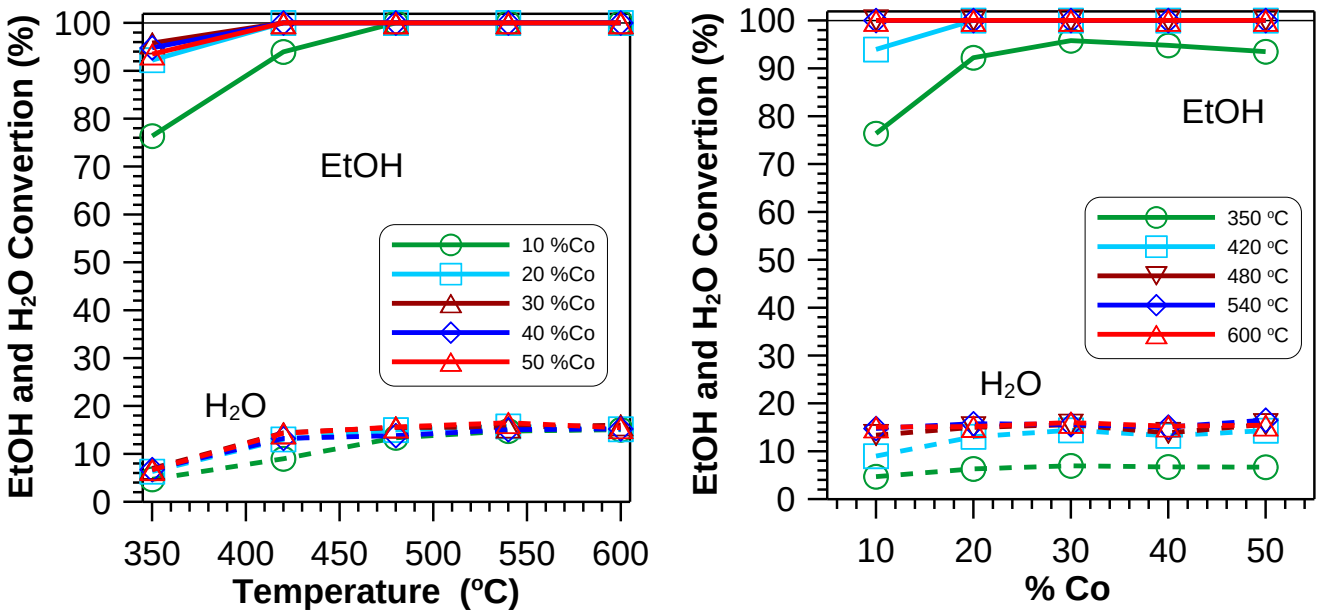

(a) (b)

Figure 4.3.7 - Effect of temperature (a) and cobalt wt% (b) in ethanol and water conversion in SRE reaction.

Neither the temperature nor the cobalt wt% has much to do with the conversion of water or ethanol. Only for lowers temperatures and lowers cobalt percentage, 350 °C and 10 wt% respectively, small decrease of ethanol conversion was observed.

In order to explain all reasons to the selectivity of the different by-products and making reference to SRE reaction itself, all reactions for the formation of hydrogen were already mentioned. So in the graphics below (figure 4.3.8) shows the selectivity to hydrogen for the different catalysts at different temperatures.

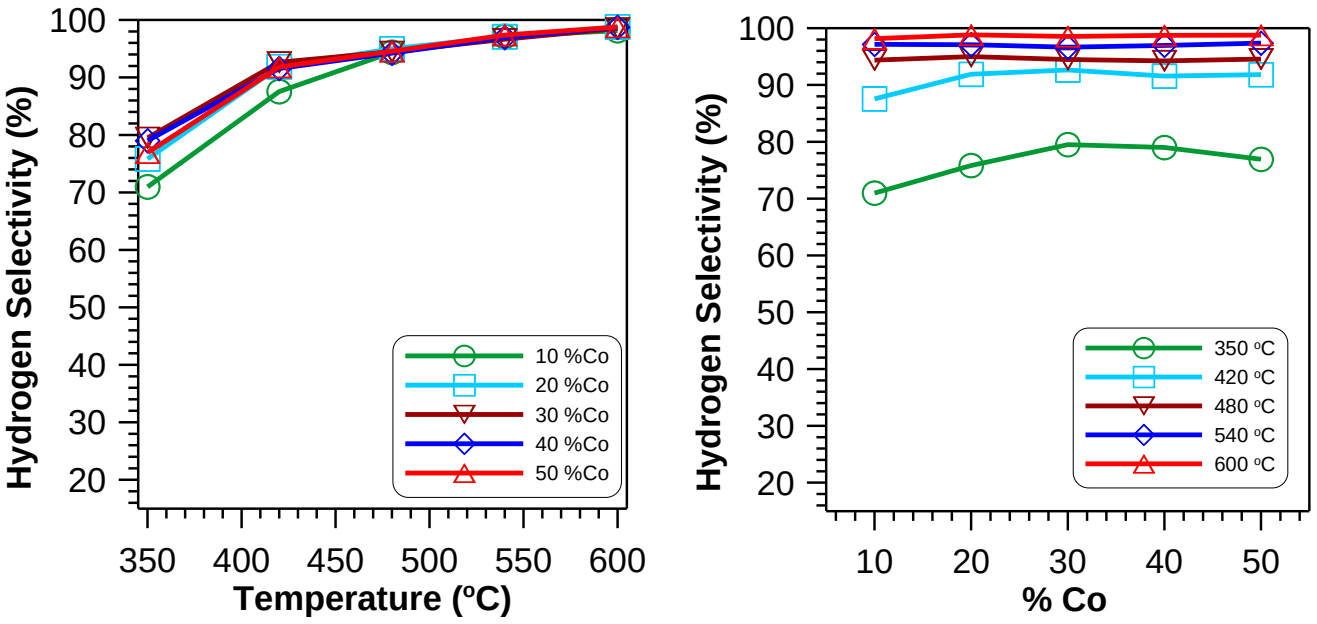

(a) (b)

Figure 4.3.8 - Effect of temperature (a) and cobalt wt% (b) in selectivity to hydrogen in SRE reaction.

In general the selectivity for hydrogen is very high and as it can be seen on the graphics, the amount of cobalt only has a small influence in his selectivity at temperatures of 350 and 420 °C being constant for higher cobalt wt%. The increase of temperature is noted with more intensity to lowers values starting to have an augment less pronounced since 480 °C to upper values, but without stop to increase with the rise of the temperature.

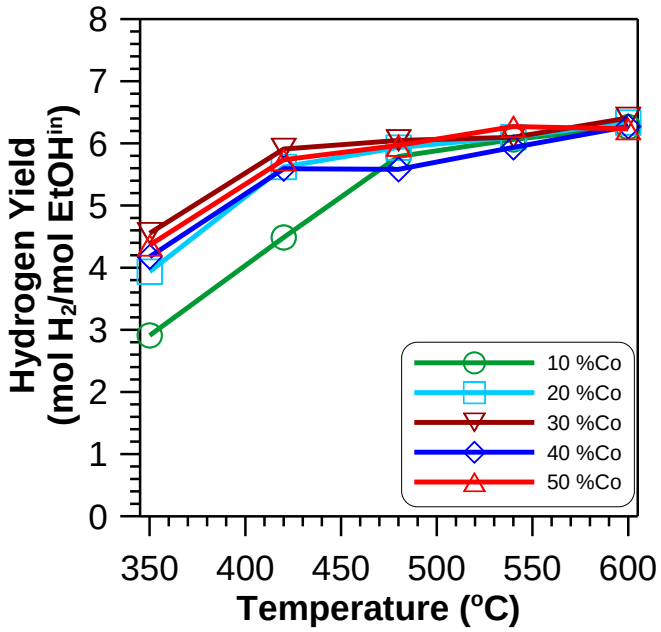

(a1)

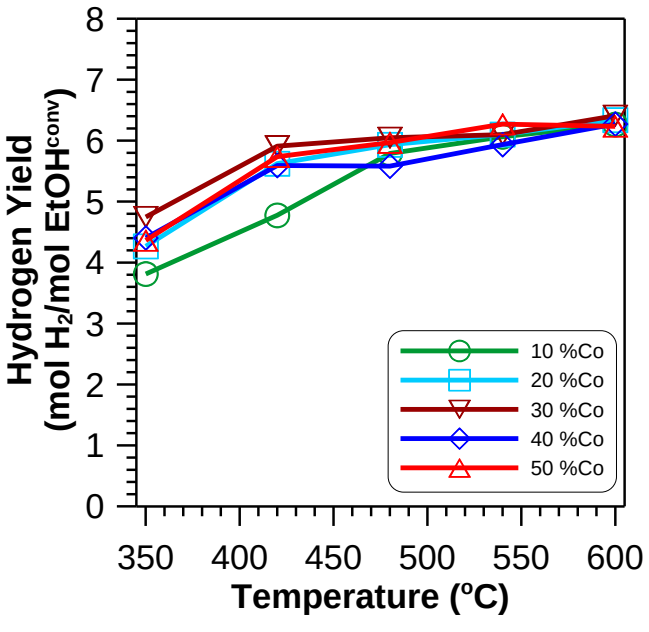

(a2)

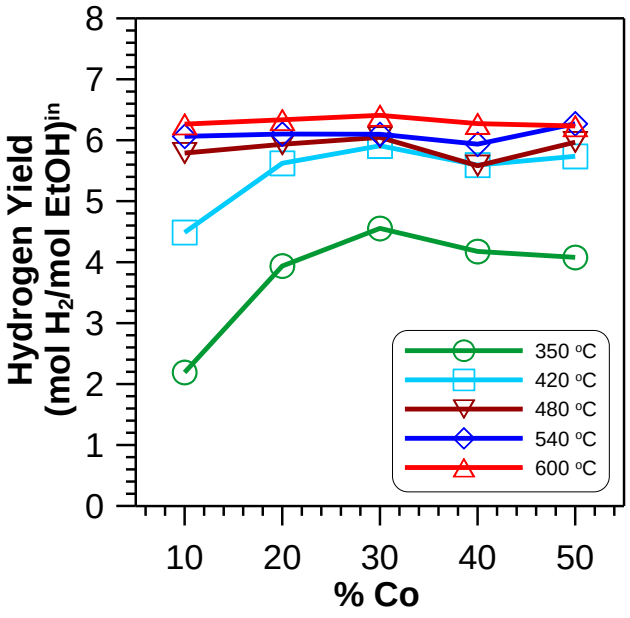

(b1)

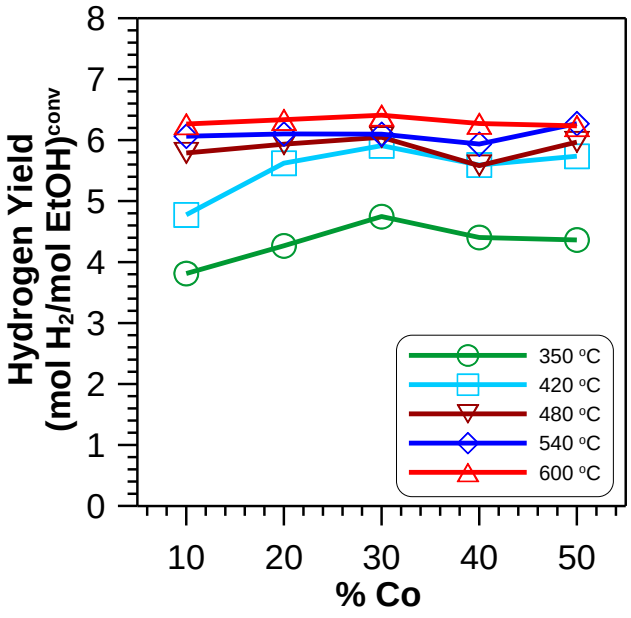

(b2)

Figure 4.3.9 - Effect of temperature (a) and cobalt wt% (b) in hydrogen yield per mol of reacted ethanol (2) and per mol of ethanol on the fed (1) in SRE reaction.

Analyzing the graphics above (figure (4.3.9)) can be seen that the hydrogen yield is almost constant to higher temperatures and has a slight reducing to temperatures below 480 °C. The cobalt wt% only has some influence to lower temperatures and above the 30 wt% is not exhibit any significant alteration in hydrogen yield. The differences illustrated between the graphics contrasting the ethanol introduced on the fed and the one that really reacted are not significant for higher temperatures and cobalt wt% because, as already seen in figure (4.3.7), at this temperature and concentrations the totality of ethanol is converted.

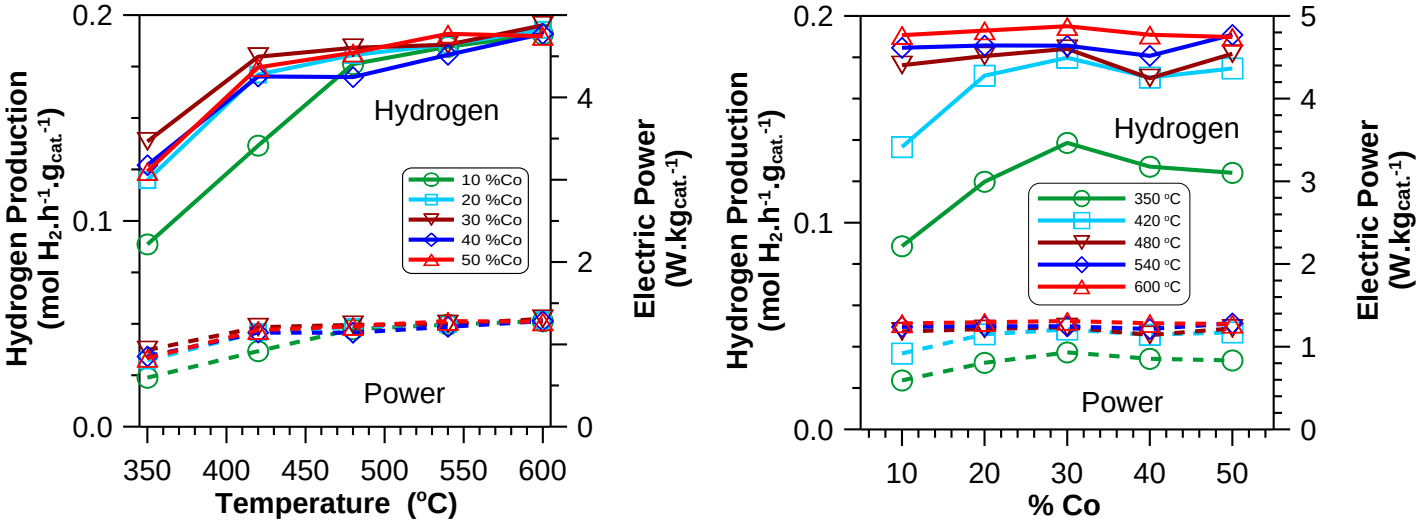

Figure 4.3.10 – Effect of temperature (a) and cobalt wt% (b) in hydrogen production with consequence amount of generated power.

The production of hydrogen is highly influenced by the temperature to low temperatures range; however for temperatures around 480 °C and higher it effect starts to decrease and the amount of hydrogen is slightly the same. With the increase of the amount of cobalt, it does not show significant divergence between the values of production, having a little decrease when used catalyst with less wt% but only a lower temperatures.

The Electric power, as predicted, varies proportionally with the hydrogen production and is only present to demonstrate the relation between both of them.

Making an analyzes more general about the results of all process and reactions involved in the steam reforming of ethanol as well the selectivity to the different formed by-products we see that the worst results, with higher amounts of undesirable products and less selectivity to hydrogen, occur for lower temperatures as 350 and 420 °C. With the exception of the selectivity to carbon monoxide that has it minimum at 420 °C, starting to increase gradually at 480 °C and having a major rise to higher temperatures.

The cobalt wt% has some influence for values of 10 and 20 wt% mainly for lower temperatures. It starting to have best results with 30 wt% and do not shows significant disparity for the catalyst with superior values of cobalt wt%. An exception has to be made to methane selectivity that have significant differences to higher amount of cobalt, having the lower selectivity to the catalyst with 50 wt%.

5 Conclusions

The co-precipitation was the chosen method to synthesize the cobalt-based catalyst and for catalysts with 10, 20 and 30 wt% a good surface area, around 100 $m^2.g^{-1}$ is exhibit, being formed by mesoporous with diameter of 18 nm approximately. A type-IV adsorption-desorption isotherm is formed with some influences of type-II, containing H3 hysteresis type loops.

Analyzing the global process of the steam reforming of ethanol, taking in account that the ideal situation was have biggest selectivity to hydrogen with less by-products as possible, we can conclude that for lower temperatures as 350 and 420 °C, the process have the largest selectivity to the by-products and the lowest to hydrogen production. So is a process that is favored at higher temperatures, however to temperatures upper than 480 °C the differences between the results are not significant and as is wanted a low-cost reformer system, the lower temperature the better. The cobalt wt% has a similar behavior, however in this case the excess of cobalt has adverse effects on the reforming.

Seeing that and knowing that reactants also cost money, the catalyst with 30 wt% in cobalt at 480 °C is the best option to be used on the steam reforming of ethanol.

However the amount of carbon monoxide produced at these conditions is still too high to be used in PEMFC.

6 References

[1] - http://www.wired.com/science/discoveries/news/2006/02/70273, visit in May 2009

[2] –Spense S, Topics in Catalysis 8 (1999) 259–266

[3] – Smelsberger T, Brown L, Boruo, International Journal of Hydrogen Energy 29 (2004) 1047 – 1064

[4] – Sun j, Qiu X, Wu F, Zhu W, Wang W, Hao S, International Journal of Hydrogen Energy 29 (2004) 1075 – 1081

[5] - Velu S, Suzuki K, Vijayaraj M, Barman S, Gopinath CHS (2005) Appl Catal B 55:287

[6] – Shen J, Song C, Catalysis Today **77** (2002) 89-98.

[7] - http://teaching.shu.ac.uk/hwb/chemistry/tutorials/chrom/chrom1.htm, visit in May 2009

[8] – Sirijaruphana A, Horváth A, Goodwin J, Oukaci R, Catalysis Letters Vol. 91, Nos. 1–2, November 2003 (2003)

[9] – Gaffron H, Rubin J, Fermentative and photochemical production of hydrogen in Algae (1942).

[10] – Benemann J, Were N, nitrogen fixation by *Anabaena cylindrical* III (1974)

[11] - Miyake J, Kawamura S, Int. J. Hydrogen Energy, 39, 147-149 (1987)

[12] – Miyake J, et al, J. Ferment. Technol, 62, 531-535 (1984)

[13] – Hofman A, introduction to modern chemistry: Experimental and theoretic. (1866)

[14] – Mattos L and Noronha F, J. Power Sources, 2005, 145, 10.

[15] –Sheng P, Yee A, Bowmaker G and Idriss H, J. Catal., 2002, 208, 393.

[16] –Lim H, Gu Y and Oyama S, Prepr. Pap.-Am. Chem. Soc., Div. Peter. Chem., 2006, 51, 31.

[17] –Cavallaro S, and Freni S, Int. J. Hydrogen Energy, 1996, 21, 465.

[18] –Diagne C, Idriss H and Kiennemann A, Catal. Commun., 2002, 3, 565.

[19] –Liguras D, Goundani K, and Verykios X, Int. J. Hydrogen Energy, 2004, 29, 419.

[20] –Cavallaro S, Chiodo V, Vita A and Freni S, J. Power Sources, 2003, 123, 10.

Appendix A – Co-precipitation calculus example

Table A1 – Molar masses for the compounds use in co-precipitation method

Compound	Molar mass ($g.mol^{-1}$)	Compound	Molar mass ($g.mol^{-1}$)	Compound	Molar mass ($g.mol^{-1}$)
Al	27.0	Zn	65.4	Co	58.9
Al_2O_3	102.0	ZnO	81.4	CoO	74.9
$Al(NO_3)_3$	375.1	$Zn(CH_3COO)_2$	219.5	$Co(CH_3COO)_2$	249.1

Amount of $Al(NO_3)_3$, in mass, to obtain 0,5 g of Al_2O_3 in the catalyst

$$m_{Al(NO_3)_3} = \frac{m_{Al} \cdot M(Al(NO_3)_3)}{Ar(Al)} \quad \text{(A.1)}$$

$$m_{Al} = \frac{0{,}5\ g\ Al_2O_3 \cdot Ar(Al_2)}{M(Al_2O_3)} \quad \text{(A.2)}$$

Amount of $Zn(CH_3COO)_2$, in mass, to obtain 9,5 g of ZnO in the catalyst

$$m_{Zn(CH_3COO)_2} = \frac{m_{Zn} \cdot M(Zn(CH_3COO)_2)}{Ar(Zn)} \quad \text{(A.3)}$$

$$m_{Zn} = \frac{9{,}5\ g\ ZnO \cdot Ar(Zn)}{M(ZnO)} \quad \text{(A.4)}$$

Amount of CoO, in mass, present in the catalyst (example for 10% of CoO)

$$\begin{aligned} 10g\ ZnO \therefore Al_2O_3 &- 90\%\ catalyst \\ x\ m_{CoO} &- 10\%\ catalyst \end{aligned}$$

Amount of $Co(CH_3COO)_2$, in mass, to obtain m_{CoO} intended in the catalyst

$$m_{Co(CH_3COO)_2} = \frac{m_{CoO} \cdot M(Co(CH_3COO)_2)}{Ar(Co)} \quad \text{(A.5)}$$

$$m_{CoO} = \frac{m_{CoO} \cdot Ar(Co)}{M(CoO)} \quad \text{(A.6)}$$

On the end was supposed to obtain between 22 and 25 g of catalyst. In order to do it and realizing that the mass of the catalyst depends also on the percentage of cobalt wanted for each sample, a adjust factor was introduced and multiplied for the mass to weight of all compounds.

Table A2 – Amount of each compound and respective adjust factor to synthesize a catalyst with 10% in cobalt oxide.

Compound	Mass to weigh (g)		Compound	Mass (g)
	Befor adjustment	After adjustment		
$Al(NO_3)_3$	3.75	7.50	CoO	1.11
$Zn(CH_3COO)_2$	25.60	51.20	$ZnO \therefore Al_2O_3$	10
$Co(CH_3COO)_2$	3.68	7.36	**Adjust Factor**	2
$CoO \therefore ZnOAl_2O_3$	11.11	22.22		

Table A3 – Amount of each compound and respective adjust factor to synthesize a catalyst with 20% in cobalt oxide.

Compound	Mass to weigh (g)		Compound	Mass (g)
	Befor adjustment	After adjustment		
$Al(NO_3)_3$	3.75	7.50	CoO	2.50
$Zn(CH_3COO)_2$	25.60	51.20	$ZnO \therefore Al_2O_3$	10
$Co(CH_3COO)_2$	3.68	16.66	**Adjust Factor**	2
$CoO \therefore ZnOAl_2O_3$	12.50	25.00		

Table A4 – Amount of each compound and respective adjust factor to synthesize a catalyst with 30% in cobalt oxide.

Compound	Mass to weigh (g)		Compound	Mass (g)
	Befor adjustment	After adjustment		
$Al(NO_3)_3$	3.75	6.38	CoO	4.29
$Zn(CH_3COO)_2$	25.60	43.52	$ZnO \therefore Al_2O_3$	10
$Co(CH_3COO)_2$	3.68	24.23	**Adjust Factor**	1.7
$CoO \therefore ZnOAl_2O_3$	14.29	24.29		

Table A5 – Amount of each compound and respective adjust factor to synthesize a catalyst with 40% in cobalt oxide.

Compound	Mass to weigh (g)		Compound	Mass (g)
	Befor adjustment	After adjustment		
$Al(NO_3)_3$	3.75	5.63	CoO	6.67
$Zn(CH_3COO)_2$	25.60	38.40	$ZnO \therefore Al_2O_3$	10
$Co(CH_3COO)_2$	22.20	33.30	**Adjust Factor**	1.5
$CoO \therefore ZnOAl_2O_3$	16.67	25.01		

Table A6 – Amount of each compound and respective adjust factor to synthesize a catalyst with 50% in cobalt oxide.

Compound	Mass to weigh (g)		Compound	Mass (g)
	Befor adjustment	After adjustment		
$Al(NO_3)_3$	3.75	4.50	CoO	10
$Zn(CH_3COO)_2$	25.60	30.72	$ZnO \therefore Al_2O_3$	10
$Co(CH_3COO)_2$	33.24	39.89	**Adjust Factor**	1.2
$CoO \therefore ZnOAl_2O_3$	20.00	24.00		

Appendix B – Brunauer-Emmett-Teller

BET theory describes quantitatively the physical adsorption of gas molecules on solids surfaces and is expressed by the following equation (B1):

$$\frac{{}^{P}/_{P_0}}{n^a\left(1-{}^{P}/_{P_0}\right)} = \frac{1}{n_m^a \cdot c} + \frac{c-1}{n_m^a \cdot c} \cdot \frac{P}{P_0} \tag{B.1}$$

P and P_0 are, respectively, the equilibrium and saturation pressures of the adsorbed gas; n_a is the quantity of gas adsorbed; n_m^a the capacity of the monolayer; and c the BET constant which is expressed by (B.2):

$$c = exp\left(\frac{E_1 - E_L}{RT}\right) \tag{B.2}$$

where, E_1 is the heat of adsorption for the first layer; and E_L is the heat of liquefaction; R is the universal gas constant; and T the temperature.

The BET equation (B.1) results on an extension of the Langmuir theory, which first expected a monolayer molecular adsorption, to a multilayer adsorption, and stands in the following hypotheses: (a) in each layer the adsorption and desorption velocities are equal; (b) from the second layer, the heat of adsorption is constant and equal to the heat of desorption; and (c) when P is equal to P_0, the steam condense as a common liquid and the number of adsorbed layers is infinity. This equation (B.1) give us a good description of experimental isotherms in a restrict range of relative pressures, usually between 0.05 and 0.3. To isotherms type-IV capillary condensation is associated a mesoporous materials but only a relative pressures quite far from the superior limit of the range, so that equation is also valid when respected the validity range.

With the aim to know the capacity of the monolayer, calculated from the experimental isotherm, a straight line was obtained by the representation of $(P/P_0)/n^a(1 - P/P_0)$ *VS* P/P_0. This line represent the BET plot and it has a slope, $\alpha = (c-1)/(n_m^a \cdot c)$ and a y-intercept, $I = 1/(n_m^a \cdot c)$, that are used to get $n_m^a = 1/(\alpha + I)$.

Acquired the capacity of the monolayer, the BET surface area, S_{BET}, can be quantified by the fowling expression (B.3):

$$S_{BET} = n_m^a \cdot N_A \cdot a_m \quad \text{(B.3)}$$

with N_A as Avogadro´s number and a_m as the area occupied by one molecule of adsorbed. The value for a_m to nitrogen at 77 K is 0.162 nm^2.

Appendix C – Barrett-Joyner-Halenda

The BJH method used to calculate PSD, accounts for capillary condensation in the pores using the modified Kelvin equation (C.1) and predicts that pore condensations changes to a higher relative pressures with the raise of temperature and pore diameter. It gives a correlation between the pore condensation pressure and his pore diameter:

$$ln\frac{P}{P_0} = -\frac{2\gamma V_L}{RTr_C} \quad \text{(C.1)}$$

γ is the surface tension; V_L is the molar volume of liquid; and $r_C = r - t(P)$ with r as the radius of the pore; and $t(P)$ as the surface layer thickness.

At the initial relative pressures of desorption process all pores are filed with the adsorbate fluid. Therefore the first step in desorption process only involves removal of capillary condensate. However, the next step involves both removal of condensate from the cores of a group of pores and the thinning of a multilayer in the larger pores (i.e. in the pores already emptied of condensate).

Appendix D – Experimental Results

Table D1 – Results from Gas Chromatography to different temperatures to catalyst with 10 wt% in cobalt.

Temperature (°C)	Number of impulses in GC									
	CO_2	C_2H_4	H_2O	CH_3CHO	C_2H_5OH	$(CH_3)_2CO$	H_2	CO	CH_4	N_2
350	480	0	39573	1212	721	29	132	431	110	18320
	402	0	40655	1166	654	29	125	378	99	17379
	311	0	40265	1253	476	22	122	375	97	17701
	303	0	40267	1258	600	21	110	332	82	17921
420	3206	3	35812	531	188	26	293	789	316	16448
	2901	3	36351	609	199	31	261	727	279	16679
	2751	4	36771	685	277	31	251	657	249	15895
480	4765	0	33395	144	0	0	375	483	327	16512
	4715	0	34509	163	0	0	374	444	306	16400
	4692	0	34216	181	0	0	370	420	299	16403
540	5395	0	32912	19	0	0	406	452	221	16065
	5446	0	33437	21	0	0	418	449	219	16221
	5396	0	33327	20	0	0	419	457	210	16164
600	5250	0	33273	11	0	0	421	598	154	16044
	5296	0	33361	7	0	0	420	574	134	16070

Table D2 – Results from Gas Chromatography to different temperatures to catalyst with 20 wt% in cobalt.

Temperature (°C)	Number of impulses in GC									
	CO_2	C_2H_4	H_2O	CH_3CHO	C_2H_5OH	$(CH_3)_2CO$	H_2	CO	CH_4	N_2
350	803	3	36885	1031	139	30	178	705	189	15039
	634	3	37413	1045	137	20	166	762	207	15380
	584	0	37075	1150	198	12	166	557	141	15107
	464	0	37970	1280	291	19	153	531	133	15109
420	4543	0	32630	51	0	0	365	448	555	15164
	4239	0	33529	127	0	0	363	469	510	14862
	4067	0	33314	119	0	0	362	516	464	14339
480	5324	0	31120	0	0	0	420	271	417	14268
	5190	0	32433	0	0	0	410	243	369	13188
540	5726	0	30136	0	0	0	443	412	238	14189
	5411	0	30385	0	0	0	436	442	228	13199
	5133	0	32561	0	0	0	433	437	240	14677
600	5305	0	31668	0	0	0	432	519	93	13162
	4987	0	32276	0	0	0	430	605	93	13824
	5110	0	32442	0	0	0	434	623	93	13346

Table D3 – Results from Gas Chromatography to different temperatures to catalyst with 30 wt% in cobalt.

Temperature (°C)	Number of impulses in GC									
	CO_2	C_2H_4	H_2O	CH_3CHO	C_2H_5OH	$(CH_3)_2CO$	H_2	CO	CH_4	N_2
	1043	3	36922	725	0	36	186	712	202	15771
350	724	0	36552	1087	152	29	170	730	207	16767
	638	0	38159	895	149	32	164	672	189	15709
	4941	0	33371	10	0	0	382	208	567	14706
420	4796	0	33537	11	0	0	383	208	553	14736
	4910	0	33679	15	0	0	384	224	564	15088
	5170	0	32125	0	0	0	413	291	473	14560
480	5451	0	32862	0	0	0	415	282	462	14977
	5296	0	33011	0	0	0	418	269	429	14242
	5888	0	31578	0	0	0	423	430	277	13957
540	5409	0	32051	0	0	0	428	429	278	13969
	5185	0	32917	0	0	0	428	424	272	14113
600	5324	0	31139	0	0	0	433	634	128	13399
	5173	0	32811	0	0	0	433	630	113	14085

Table D4 – Results from Gas Chromatography to different temperatures to catalyst with 40 wt% in cobalt.

Temperature	Number of impulses in GC									
(°C)	CO_2	C_2H_4	H_2O	CH_3CHO	C_2H_5OH	$(CH_3)_2CO$	H_2	CO	CH_4	N_2
350	1309	5	36132	787	0	36	205	892	257	16393
	1008	0	36921	1040	144	20	190	690	197	14620
	662	3	38919	1069	258	0	178	716	200	15953
420	4836	0	33751	0	0	0	385	159	645	13904
	4909	0	33982	0	0	0	387	142	602	14199
480	5582	0	32878	0	0	0	413	255	461	14009
	5344	0	33076	0	0	0	423	265	465	14507
	5528	0	32817	0	0	0	421	236	420	14389
540	5893	0	32059	0	0	0	455	428	255	13957
	5476	0	32372	0	0	0	455	449	253	13367
	5554	0	32723	0	0	0	449	440	239	13644
600	5202	0	32407	0	0	0	454	641	103	14116
	5380	0	32808	0	0	0	456	639	103	13861

Table D5 – Results from Gas Chromatography to different temperatures to catalyst with 50 wt% in cobalt.

Temperature (°C)	Number of impulses in GC									
	CO_2	C_2H_4	H_2O	CH_3CHO	C_2H_5OH	$(CH_3)_2CO$	H_2	CO	CH_4	N_2
350	914	5	37048	915	178	0	185	846	236	15938
	670	4	38204	1071	166	0	177	701	195	15536
	610	7	38376	1382	158	0	172	620	180	15123
420	4908	0	32996	3	0	0	388	134	653	14435
	5037	4	33196	0	0	0	396	162	623	13927
	5072	0	33372	0	0	0	397	163	625	14579
480	5493	0	32805	0	0	0	434	291	464	14263
	5444	0	33233	0	0	0	444	285	451	13678
	5639	0	32417	0	0	0	443	290	463	14051
540	5987	0	31394	0	0	0	474	458	240	13109
	5650	0	32069	0	0	0	462	452	220	13279
	5345	0	32615	0	0	0	457	459	223	13822
600	5429	0	32284	0	0	0	442	647	105	13122
	5378	0	32365	0	0	0	452	658	97	13627

Appendix E – SRE Calculus Example

Ethanol Conversion

Every calculation done to reach the values of conversion for ethanol and water, were made on the basis of their concentrations before and after the reaction. As they were based on the volume percentage, and it changes during the reaction, a correction factor was introduced in order to minimize the errors.

The ethanol conversion, X_A, is given by the following equation:

$$X_A = \frac{C_A^{in} - C_A^{out} \cdot K}{C_A^{in}} \cdot 100 \quad \text{(E.1)}$$

where, C_A^{in} and C_A^{out} are, respectively, the molar concentrations of ethanol in the reaction mixture and in steam products; and K the volum contraction factor, given by the ratio between the molar concentration of carbon in ethanol fed and the molar concentration of carbon in all carbon-containing compound in products, equation (E.2):

$$K = \frac{C_C^{in}}{C_C^{out}} = \frac{2C_A^{in}}{f_C} \quad \text{(E.2)}$$

with f_C as the total percentage volume of product compounds which contains carbon in his structure; it is calculated from the following expression (E.3):

$$f_C = \sum_{i=0}^{n} \left(x \cdot C_i^{out} \right) \quad \text{(E.3)}$$

with n as the number of the different compounds on the stream of products; x as the number of carbon atoms present on each compound; and C_i^{out} as the concentration, in percentage of volume, of the compound i.

Equation can be rearranged in other way, originating other formula to calculate the ethanol conversion. So, Multiplicand both members of the equation for f_C/C_A^{in}, we get the following expression:

$$X_A = \frac{f_C - 2C_A^{in}}{f_C} \cdot 100 \quad \text{(E.4)}$$

The concentration of the compound on the post-reaction mixture is also based in an adjustment (E.5):

$$C_i^{out} = \frac{C_i^{out\,*}}{C_T^{out}} \cdot 100 \quad \text{(E.5)}$$

being i any compound obtained after SRE, $C_A^{out\,*}$,for example, is the concentration of ethanol before the adjustment; this kind of adjustment has to be made because of the existence of another nitrogen stream right on the end of the reactor, to help carry out the products up to the GCs. As this concentration is on percentage of volume, the extra volume of nitrogen has to be included; C_T^{out} is the sum of the concentration, before adjustment, of all n products recovered from the reactor (W.3):

$$C_T^{out} = \sum_{i=0}^{n} C_i^{out\,*} \quad \text{(E.6)}$$

The concentration of each product identified in Varian CP-3800 is calculated from the following expression (E.6):

$$C_i^{out\,*} = \frac{S_i}{\lambda_i \cdot W_{N_1}} \cdot 100 \quad \text{(E.7)}$$

that is based on the number of impulses, or the area of the peak, for compound i, S_i per the number of impulses of nitrogen standard, W_{N_1}. Is also introduced a correction factor, λ_i, to counterbalance some eventual flaw from the GC and its obtained dividing the number of impulses of the respective compound standard, W_i, per the number of impulses of nitrogen standard:

$$\lambda_i = \frac{W_i}{W_{N_1}} \quad \text{(E.8)}$$

Hydrogen concentration does not need the correction factor to be calculated and it expression is described below (E.9):

$$C_H^{out\ *} = \frac{S_H}{W_{N_2}} \cdot 100 \quad \text{(E.9)}$$

When it makes some references for standard number of impulses, it refers to making a reading on the GC with the afore-mentioned product in the pure form, in other words, without the interference of other compounds and knowing the exact amount introduced in the GC. In respect of the nitrogen, as it is the carrier gas for both GC apparatus, two different measures have to be made, one for each apparatus and we will have W_{N_1} to Varian CP-3800 and W_{N_2} to GCHF 18.3.

Water Conversation

Analogous to the reasoning made to ethanol conversation, for water conversion, X_W the expression has the following appearance:

$$X_W = \frac{C_W^{in} - C_W^{out} \cdot K}{C_W^{in}} \cdot 100 \quad \text{(E.10)}$$

where, C_w^{in} and C_w^{out} are, respectively, the molar concentrations of water in the reaction mixture and in steam products

So applying the same methodology that in the conversion of ethanol, equation (E.10) can be written as it is below:

$$X_W = \frac{f_H - 3f_C - 2C_W^{out}}{f_H - 3f_C} \cdot 100 \quad \text{(E.11)}$$

C_W^{out} can be calculated with equation (E.5) and f_H is the total percentage volume of product compounds which contains hydrogen in his structure:

$$f_H = \sum_{i=0}^{n} \left(x \cdot C_i^{out} \right) \quad \text{(E.12)}$$

with n as the number of the different compounds on the stream of products; x as the number of hydrogen atoms present on each compound, i.

Selectivity

For hydrogen selectivity was used the equation (G.1) represented below:

$$Sel_H = \frac{2C_H^{out}}{\sum_{i=0}^{n}(x \cdot C_i^{out})} \cdot 100 \quad \text{(E.14)}$$

n is the number of the different products of SRE; x is the number of hydrogen atoms present on each compound, i.

For all the rest of the SRE´s products the used expression is:

$$Sel_i = \frac{x \cdot C_i^{out}}{f_C - 2C_A^{out}} \cdot 100 \quad \text{(E.15)}$$

where x is the number of carbon atoms present on the compound, i.

Electrical Power

The all goal to produce hydrogen is to soon after produce electrical power from hydrogen in PEMFCs. The following expressions can give a relation between the amount of hydrogen produced and the electrical power generated in W/kg_{cat}.

$$Power = F_A \cdot H/A_0 \cdot 67.18 \quad \text{(E.16)}$$

where F_A is the flow of ethanol in $mol.h^{-1}$; H/A_0 is the amount of hydrogen which is produced per mol ethanol introduced on the fed in mol H_2/mol $_{Ethanol}$; and the value 67.18 is based on calculations from the enthalpy for hydrogen combustion reaction.

$$H/A_0 = \frac{H/A_t \cdot X_A}{100} \quad \text{(E.17)}$$

where H/A_t is the amount of hydrogen which is produced per mol of reacted ethanol in mol H_2/mol $_{Ethanol}$ and is given by the following expression:

$$H/A_t = \frac{2C_H^{out}}{f_C - 2C_A^{out}} \quad \text{(E.18)}$$

The ethanol flow can be calculated from equation (E.19):

$$F_A = \frac{F_T \cdot mol_A}{mol_T} \quad \text{(E.19)}$$

where F_T is the total flow that enters on the reactor; mol_A is the number moles of ethanol in the fed; and mol_A is the number of total moles on the fed.

$$P_{H_2} = \frac{H/A_0 \cdot F_A}{m_{Cat}} \quad \text{(E.20)}$$

The equation (E.20) above is representative of the productivity of hydrogen in mol H_2.h^{-1}.g^{-1}.

Appendix F – Results of SRE

Table F1 – Values obtained to construct the graphics that illustrate what happens in the SRE at 350 °C to the different catalyst.

Wt %	X_A	X_W	Selectivity							H/A_t	H/A_0	P_{H_2}	Power
			CH_4	CO	CO_2	C_2H_4	CH_3CHO	$(CH_3)_2CO$	H_2				
10	76.37	4.68	3.99	13.26	12.89	0.00	68.26	1.60	70.97	3.8122	2.1907	0.0886	0.59185
20	92.22	6.31	5.98	19.41	18.62	0.09	54.80	1.11	75.82	4.2663	3.9370	0.1198	0.80505
30	95.78	6.95	7.28	21.87	24.56	0.06	44.41	1.82	79.50	4.7460	4.5528	0.1386	0.93097
40	94.80	6.72	7.15	21.38	27.07	0.14	43.36	0.90	78.99	4.4041	4.1751	0.1271	0.85373
50	93.48	6.67	6.90	20.81	20.79	0.30	51.20	0.00	76.91	4.3633	4.0776	0.1241	0.83380

Table F2 – Values obtained to construct the graphics that illustrate what happens in the SRE at 420 °C to the different catalyst.

Wt %	X_A	X_W	Selectivity							H/A_t	H/A_0	P_{H_2}	Power
			CH_4	CO	CO_2	C_2H_4	CH_3CHO	$(CH_3)_2CO$	H_2				
10	93.95	8.98	6.61	14.47	58.26	0.13	19.46	1.06	87.55	4.7746	4.4872	0.1366	0.91776
20	100.00	13.03	10.96	8.77	77.36	0.00	2.91	0.00	91.88	5.6222	5.6222	0.1711	1.14966
30	100.00	14.38	11.56	3.73	84.37	0.00	0.33	0.00	92.64	5.9082	5.9082	0.1798	1.20814
40	100.00	13.23	12.88	2.64	84.47	0.00	0.00	0.00	91.56	5.5922	5.5922	0.1702	1.14351
50	100.00	14.31	12.76	2.62	84.55	0.04	0.03	0.00	91.81	5.7361	5.7361	0.1746	1.17294

Table F3 – Values obtained to construct the graphics that illustrate what happens in the SRE at 480 °C to the different catalyst.

Wt %	X_A	X_W	Selectivity							H/A_t	H/A_0	P_{H_2}	Power
			CH_4	CO	CO_2	C_2H_4	CH_3CHO	$(CH_3)_2CO$	H_2				
10	100.00	13.36	6.37	7.82	81.29	0.00	4.52	0.00	94.37	5.7883	5.7883	0.1762	1.1836
20	100.00	14.98	7.82	4.35	87.83	0.00	0.00	0.00	94.99	5.9329	5.9329	0.1806	1.2132
30	100.00	15.53	8.84	4.64	86.52	0.00	0.00	0.00	94.47	6.0474	6.0474	0.1841	1.2366
40	100.00	13.82	8.52	4.07	87.41	0.00	0.00	0.00	94.24	5.5822	5.5822	0.1699	1.1415
50	100.00	15.62	8.60	4.59	86.80	0.00	0.00	0.00	94.55	5.9685	5.9685	0.1817	1.2205

Table F4 – Values obtained to construct the graphics that illustrate what happens in the SRE at 520 °C to the different catalyst.

Wt %	X_A	X_W	Selectivity							H/A_t	H/A_0	P_{H_2}	Power
			CH_4	CO	CO_2	C_2H_4	CH_3CHO	$(CH_3)_2CO$	H_2				
10	100.00	14.76	4.19	7.44	87.84	0.00	0.52	0.00	97.15	6.0643	6.0643	0.1846	1.24006
20	100.00	15.75	4.58	7.12	88.31	0.00	0.00	0.00	97.09	6.1012	6.1012	0.1857	1.24760
30	100.00	15.56	5.26	6.94	87.80	0.00	0.00	0.00	96.66	6.0977	6.0977	0.1856	1.24689
40	100.00	15.04	4.65	6.98	88.37	0.00	0.00	0.00	96.96	5.9352	5.9352	0.1807	1.21366
50	100.00	16.50	4.25	7.24	88.51	0.00	0.00	0.00	97.36	6.2712	6.2712	0.1909	1.28238

Table F5 – Values obtained to construct the graphics that illustrate what happens in the SRE at 600 °C to the different catalyst.

Wt %	X_A	X_W	Selectivity							H/A_t	H/A_0	P_{H_2}	Power
			CH_4	CO	CO_2	C_2H_4	CH_3CHO	$(CH_3)_2CO$	H_2				
10	100.00	15.05	2.84	9.81	87.12	0.00	0.24	0.00	98.15	6.2650	6.2650	0.1907	1.28111
20	100.00	15.15	1.90	10.12	87.98	0.00	0.00	0.00	98.81	6.3366	6.3366	0.1929	1.29573
30	100.00	16.00	2.38	10.61	87.01	0.00	0.00	0.00	98.54	6.4080	6.4080	0.1950	1.31034
40	100.00	15.23	2.03	10.70	87.28	0.00	0.00	0.00	98.72	6.2733	6.2733	0.1909	1.28280
50	100.00	15.44	1.95	10.69	87.37	0.00	0.00	0.00	98.77	6.2348	6.2348	0.1898	1.27492